UNIVERSITY OF TURKU
Faculty of Science

Effects of *CASP8* mutations on radiotherapy and inflammatory responses in cancer cells

Meri Pelkonen

Physiology and Genetics
Master's thesis
Credits: 30 op

Supervisors:
Kari Kurppa
Päivi Koskinen

25.5.2023
Turku

Master's thesis

Subject: Biology, Physiology and Genetics
Author: Meri Pelkonen
Title: Effects of *CASP8* mutations on radiotherapy and inflammatory responses in cancer cells
Supervisors: Kari Kurppa, Päivi Koskinen
Number of pages: 57 pages + 1 appendix
Date: 25.5.2023

CASP8 mutations occur most commonly in head and neck squamous cell carcinoma (HNSCC), with a mutation frequency of 10,7 %. Alterations in this gene have been shown to impair the effects of radiotherapy in HNSCC patients and are associated with poor overall survival. Thus, it is of great importance to identify the means cancer cells use to escape cell death and develop resistance to cancer therapies in order to find predictive markers. Caspase-8 is a cysteine protease, encoded by the *CASP8* gene that plays a crucial role in both extrinsic apoptosis and inflammatory signaling, while acting as an inhibitor of necroptosis. In apoptotic signaling, the catalytic activation of Caspase-8 by cleavage and dimerization is required, while in inflammatory signaling, procaspase-8 acts as a scaffold for FADDosome formation independently from its catalytic activity.

CASP8 mutations have a complex role in HNSCC; mutations have been shown to impair and inhibit death receptor-mediated cell death as well as to promote activation of NF-κB-dependent inflammatory signaling. Previous studies have shown that HNSCC-associated *CASP8* mutations could inhibit the activation of apoptotic signaling and cell death following death receptor stimulation. Moreover, mutations have been shown to both impair and enhance the NF-κB-dependent inflammatory signaling, depending on the mutation site. These findings indicate the diverse functional properties of HNSCC-associated *CASP8* mutations, rather than only being loss-of-function mutations.

This thesis aimed to investigate the contributions of nine HNSCC-associated *CASP8* mutations (L7V, L62P, R71T, S99F, L105H, D303G, S375*, T441I and Q465*) to radiotherapy response in cancer cells. In addition, the effects of *CASP8* mutations on inflammatory signaling mediated by death receptor stimulation in cancer cells were studied. *CASP8* mutations were generated by site-directed mutagenesis and cloned using Gateway cloning. HeLa $^{CASP8-/-}$ cells were then virally transduced with mutation plasmids. Created stable *CASP8* mutation cell lines were irradiated, after which cell viabilities were measured using the MTT assay. The effects of *CASP8* mutations on the cytokine and chemokine expression following irradiation and TRAIL treatment were analysed by qPCR.

Based on the findings from this study, mutations T441I and Q465* exhibited higher cell viability following irradiation compared to WT CASP8, suggesting that these mutations could potentially impair the activation of cell death signaling after irradiation. Moreover, seven out of nine CASP8 mutants were more sensitive to irradiation than WT CASP8. This study also showed that most of the CASP8 mutants retained their ability to activate NF-κB-dependent inflammatory signaling following irradiation or death receptor stimulation by TRAIL. However, further studies are required to determine whether mutations T441I and Q465* have potential to act as predictive markers in HNSCC.

Key words: *CASP8*, HNSCC, mutation, irradiation, cell death, NF-κB, cancer therapy resistance, predictive marker

Pro gradu -tutkielma

Pääaine: Biologia, Fysiologian ja genetiikan linja
Tekijä: Meri Pelkonen
Otsikko: *CASP8* mutaatioiden vaikutukset sädetys- ja tulehdusvasteeseen syöpäsoluissa
Ohjaajat: Kari Kurppa, Päivi Koskinen
Sivumäärä: 57 sivua + 1 liitesivu
Päivämäärä: 25.5.2023

CASP8 mutaatioita esiintyy yleisimmin pään ja kaulan levyepiteelikarsinoomassa, jossa geenin mutaatiofrekvenssi on 10,7 %. Näiden muutosten on osoitettu heikentävän sädehoidon vaikutuksia syöpäpotilailla sekä korreloivan potilaiden huonon eloonjäämisen kanssa. Siksi on erittäin tärkeää tunnistaa mekanismit, joiden avulla syöpäsolut välttävät solukuoleman ja kehittävät vastustuskykyä syöpähoitoja vastaan. Tunnistamalla nämä tekijät voitaisiin kehittää markkereita ennustamaan potilaiden hoitovastetta. Kaspaasi-8 on *CASP8*-geenin koodaama kysteiiniproteaasi, joka osallistuu apoptoosiin sekä tulehdukselliseen signalointiin, samalla inhiboiden nekroptoosia. Kaspaasi-8 aktivoituu proentsyymin (prokaspaasi-8) pilkkoutumisen ja dimerisaation seurauksena ja katalyyttisesti aktiivinen kaspaasi-8 on olennainen osa apoptoosin signalointia. Tulehduksellisessa signaloinnissa ei vaadita kaspaasi-8:n aktivaatiota, vaan prokaspaasi-8 molekyylit toimivat telineenä FADDosomin muodostumiselle.

CASP8 mutaatioilla on erilaisia funktionaalisia ominaisuuksia ja vaikutuksia erityisesti pään ja kaulan levyepiteelikarsinoomassa; mutaatioiden on osoitettu heikentävän ja estävän kuolonreseptorivälitteistä solukuolemaa sekä edistävän NF-κB-riippuvaista tulehduksellista signalointia. Aiemmat tutkimukset ovat osoittaneet, että pään ja kaulan levyepiteelikarsinoomassa havaitut *CASP8* mutaatiot voivat estää solukuoleman signalointia ja siten apoptoosia. Lisäksi mutaatioiden on osoitettu sekä heikentävän että tehostavan NF-κB-riippuvaista tulehduksellista signalointia mutaation sijainnista riippuen. Nämä havainnot osoittavat *CASP8* mutaatioiden erilaiset funktionaaliset ominaisuudet syövässä sen sijaan, että koko geenin toiminta olisi menetetty.

Tämän pro gradu- tutkielman tarkoituksena oli tutkia yhdeksän *CASP8* mutaation (L7V, L62P, R71T, S99F, L105H, D303G, S375*, T441I ja Q465*) vaikutusta syöpäsolujen sädehoitovasteeseen. Lisäksi tutkittiin *CASP8* mutaatioiden vaikutuksia kuolonreseptorin välittämään tulehdukselliseen signaloitiin syöpäsoluissa. *CASP8* mutaatiot luotiin kohdennetulla mutageneesillä ja Gateway-kloonauksen sekä lentivirus transduktion avulla mutaatiot siirrettiin HeLa $^{CASP8-/-}$ soluihin. Mutaatiosolulinjoja säteilytettiin, minkä jälkeen solujen viabiliteeti mitattiin MTT:llä. *CASP8* mutaatioiden vaikutuksia sytokiinien ja kemokiinien ilmentymiseen säteilytyksen ja TRAIL:n jälkeen analysoitiin qPCR:llä.

Tämän tutkielman tulosten perusteella mutaatiot T441I ja Q465* osoittivat parempaa viabiliteettia säteilytyksen jälkeen kuin villityypin kaspaasi-8, viitaten siihen, että nämä mutaatiot mahdollisesti heikentäisivät kuolonsignalointia säteilytyksen jälkeen. Lisäksi seitsemän yhdeksästä CASP8-mutantista olivat herkempiä säteilylle kuin villityypin kaspaasi-8. Tämä tutkimus osoitti myös, että lähes kaikki tutkitut *CASP8* mutaatiot säilyttivät kyvyn aktivoida NF-κB-riippuvaista tulehduksellista signalointia säteilytyksen tai TRAIL-käsittelyn jälkeen. Jatkotutkimuksia tarvitaan kuitenkin selvittämään, voisivatko mutaatiot T441I ja Q465* mahdollisesti toimia predikatiivisina markkereina pään ja kaulan levyepiteelikarsinoomassa.

Avainsanat: *CASP8*, pään ja kaulan levyepiteelikarsinooma, mutaatio, sädetys, solukuolema, NF-κB, syöpähoitoresistenssi, predikatiivinen markkeri

List of abbreviations

ANOVA	analysis of variance
$cFLIP_{S/L}$	FLICE-like inhibitory protein short/long
cIAP	cellular inhibitor of apoptosis
CXCL1	chemokine (C-X-C motif) ligand 1
CYLD	ubiquitin carboxyl-terminal hydrolase
DD	death domain
DED	death effector domain
DISC	death-inducing signaling complex
FADD	Fas-associated death domain
HNC	head and neck cancer
HNSCC	head and neck squamous cell carcinoma
HPV	human papilloma virus
IKK	IκB kinase
IL-6	interleukin 6
IL-8	interleukin 8
IPM	induced-proximity model
IR	ionizing radiation
KO	knock-out
MAPK	mitogen-activated protein kinase
MLKL	mixed lineage kinase domain like
NF-κB	nuclear factor kappa B
OSCC	oral squamous cell carcinoma

RCV	replication-competent lentivirus
RIPK	receptor-interacting protein kinase
ROS	reactive oxygen species
TAB	TAK-binding protein
TAK	transforming growth factor β-activated kinase
TCGA	The Cancer Genome Atlas
TME	tumor microenvironment
TNF	tumor necrosis factor
TNF-R	TNF receptor
TRADD	TNF-R associated death domain
TRAF	TNF-R-associated factor
TRAIL	TNF-related apoptosis inducing ligand
WT	wild-type

Contents

1 Introduction

1.1 Head and neck squamous cell carcinoma

1.1.1 Epidemiology

Head and neck cancer (HNC) is the seventh most common cancer worldwide (Sung et al. 2021). HNC refers to malignant tumors that are located in the mouth or throat, larynx, nose and sinuses. In 2020, 660 000 new cases of HNC were reported with a mortality rate of ~50 % (Sung et al. 2021). However, the 5-year survival rate has increased to 66 % in the beginning of the 21st century (Pulte & Brenner 2010). Approximately 90 % of the HNCs are squamous cell carcinomas (Sung et al. 2021) derived from the mucosal epithelium of oral cavity, pharynx (naso-, oro- and hypopharynx) or larynx (Johnson et al. 2020). Head and neck squamous cell carcinomas (HNSCC) are two to four times more common within male population than in females, most likely due to sex-specific patterns of risk behaviors (Johnson et al. 2020). HNSCC significantly affects the quality of patient's life even long after treatments. Approximately 50 % of HNSCC survivors suffer from swallowing and speech problems after chemoradiation therapy (Rinkel et al. 2016).

1.1.2 Development and genomic alterations in HNSCC

Risk factors for HNSCC are tobacco (both smoked and non-smoked) and alcohol consumption, infection with the human papilloma virus (HPV), as well as exposure to environmental pollutants (Wong et al. 2014). Cancers arising from the oral cavity and larynx are usually associated with tobacco and alcohol consumption, whereas pharynx cancers are usually caused by infection with HPV (Isayeva et al. 2012; Stein et al. 2015). General aging, poor oral hygiene and vegetable-poor diets are also risk factors for developing HNSCC (Guha et al. 2007; Freedman et al. 2008). In addition, genetic polymorphism in genes that are involved in carcinogenic metabolism and immunity can contribute to arising of HNSCC (Cadoni et al. 2012). Altogether, contribution of each risk factor in HNSCC can be difficult to assess since they are strongly related to each other.

HNSCC arises from the mucosal epithelium that consists of two layers: surface squamous epithelium and the deeper lamina propria, an underlying connective tissue. Originally in 1996, Califano et al. described that the development of HNSCC begins with epithelial cell hyperplasia (increased amount of cells in tissue), leading to dysplasia (presence of

abnormal cells within a tissue), and carcinoma in situ, eventually leading to invasive carcinoma. Many genomic alterations can promote the development of HNSCC. In HPV-negative HNSCC, accumulation of alterations especially in tumor suppressor genes *TP53* and *CDKN2A* and in other signaling pathways are associated with the development and poor prognosis of HNSCC (Johnson et al. 2020). Findings from an HNSCC patient sample whole exome analysis by Stransky et al. (2011) supported discoveries of *CDKN2A* inactivation and amplification of *CCND1* in HNSCC, and also resulted in finding of novel *NOTCH1* mutations in human squamous malignancies. In addition, they discovered that *CASP8* alterations were detected in HNSCC patients, indicating that suppression of apoptosis may contribute to the development of malignancies.

1.1.3 Radiotherapy as treatment in HNSCC

Biopsies of primary tumors and HPV testing are used for diagnosis of HNSCC. HPV-negative HNSCCs are usually diagnosed in the median age of 66, whereas HPV-positive cancer cases are diagnosed around the median age of 53 years (Johnson et al. 2020). The treatments of HNSCC include resection, radiation and systemic therapy, depending on the location of the tumor, while ensuring organ-preservation approach. According to the Cancer Genome Atlas, TCGA, irradiation is the most commonly used therapy for HNSCC (Cerami et al. 2012; Gao et al. 2013). Radiotherapy kills cancer cells by inducing irreparable DNA damage. Radiotherapy is used for 60% of cancer patients with solid tumors (Prasanna et al. 2014), and is a commonly used treatment in HNSCC due to the possibility of organ preservation. The desirable result of radiotherapy is to kill as many tumor cells as possible and thereby decrease tumor growth and prevent metastases. Ionizing radiation (IR) induces extrinsic and intrinsic apoptotic cell death as well as membrane apoptotic signaling, i.e. ceramide production (Rahmanian et al. 2016). In addition to the apoptotic pathways, irradiation can induce cancer cell death through necroptosis and autophagy (Palumbo & Comincini 2013; Rahmanian et al. 2016).

Irradiation generates reactive oxygen species (ROS) and free radicals and therefore causes DNA damage in the genome. Most commonly it causes double-stranded breaks which are among the most toxic DNA lesions (Roos & Kaina 2013). DNA damage leads to activation of DNA repair mechanisms, such as activation of the tumor suppressor gene *TP53*. Induced expression of P53 leads to transactivation of death receptors and further recruitment of DISC (Death-Inducing Signaling Complex), resulting in caspase cascade

activation (as described in Chapter 1.2.1). In addition to death receptor activation, activation of P53 also results in transactivation of the death receptor ligands (Maier et al. 2016; Rahmanian et al. 2016).

HNSCC patient data illustrates that *CASP8* alterations have a significant effect on the overall survival of patients when they are solely treated with radiotherapy (Fig 1.). *CASP8* mutations have been shown to impair the response of cancer therapies that are based on death receptor-induced cell death (Li et al. 2014; Cui et al. 2021), raising the question of whether *CASP8* alterations could confer resistance to radiotherapy in HNSCC patients. Treatment resistance in cancer patients could also be correlated to heterogenous tumor microenvironment (Prasanna et al. 2014). Surely, many factors can affect therapy resistance, such as the stage and location of the tumor as well as the heterogeneity, thus it is important to identify the possible limiting factors in cell death sensitivity and radiotherapy resistance.

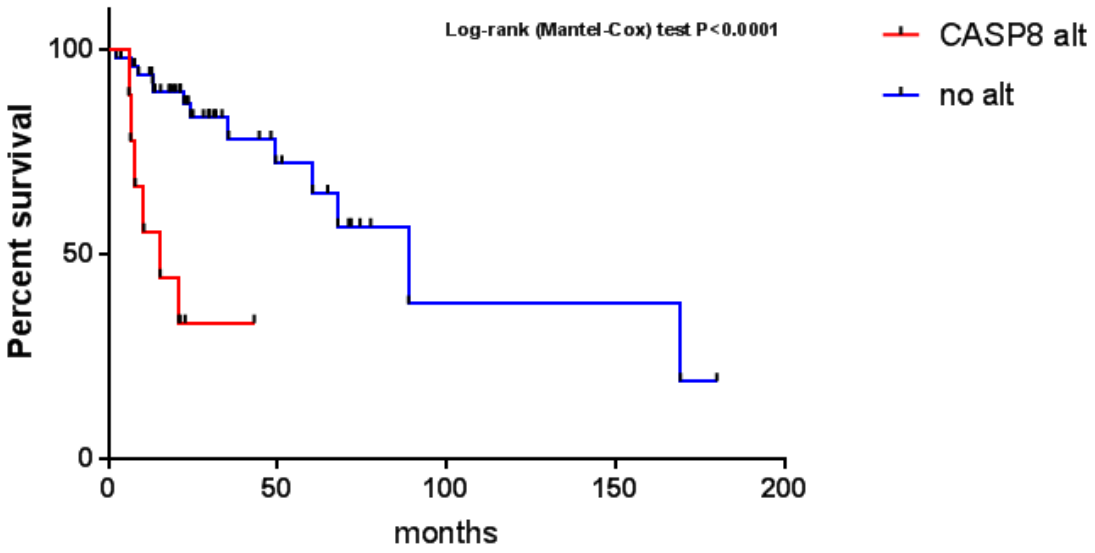

Figure 1. Overall survival of HNSCC patients. *CASP8* alterations have a significant effect on the prognosis of HNSCC patients when they are treated with radiotherapy alone. Red line represents HNSCC patients with *CASP8* alterations (CASP8 alt) while the blue line represents cancer patients with non-mutated *CASP8* (no alt). Retrieved from cBioPortal, TCGA & PanCancer Atlas 11/2022 (Cerami et al. 2012, Gao et al. 2013).

1.2 Caspase-8

Caspases are highly conserved and are found in almost every mammalian cell (Mandal et al. 2020). They are cysteine proteases specific for aspartate, the substrate specificity of which is determined by the amino acid sequence that precedes the aspartic acid cleavage site of the substrate. Caspases are key elements in programmed cell death, both in extrinsic and intrinsic apoptosis. Apoptosis is an important cellular event that is involved in embryonal development, protection against infections and pathogens as well as continuous elimination of cells that have reached the end of their lifespan. Avoiding and resisting cell death is one of the hallmarks of cancer cells (Hanahan 2022).

Caspase-8 plays a crucial role in both extrinsic apoptosis and inflammatory signaling. However, the difference between these roles of Caspase-8 lies in its catalytic activity. Catalytic activity of Caspase-8 is required for apoptotic signaling while in inflammatory signaling, Caspase-8 acts as a scaffold independent from its catalytic activity (Henry & Martin, 2017). Caspase-8 is also involved in other cell death pathways such as intrinsic apoptosis and pyroptosis, while acting as an inhibitor of necroptosis (Orning & Lien 2021). Caspase-8 is encoded by the *CASP8* gene which is located in the chromosome 2 longer arm in location of 33.1 (2q33.1), and consists of 16 exons. Caspase-8 is synthesized in a zymogen form, procaspase-8, and its activation requires both dimerization and cleavage.

Procaspase-8 consists of an N-terminal prodomain and a C-terminal protease domain, including linker regions between these two domains (Watt et al. 1999). The prodomain is formed by two death effector domains, DED1 and DED2, both possessing a crucial role in interaction with adaptor proteins. The catalytic protease domain of procaspase-8 consists of large and small subunits, p18 and p10, respectively. Alternative splicing of *CASP8* results in multiple isoforms of procaspase-8, but only two isoforms, procaspase-8 a and b, are known to be functional in apoptosis (Mandal et al. 2020).

1.2.1 Caspase-8 in extrinsic apoptosis

Extrinsic apoptotic signaling is initiated by activation of death receptors, leading to receptor aggregation, recruitment of adaptor proteins and activation of an apical initiator caspase, which in turn activates the caspase cascade and eventually leads to programmed

cell death, apoptosis. Death receptors belong to the tumor necrosis factor (TNF) superfamily which comprises of 29 members. These transmembrane proteins consist of a C-terminal intracellular tail, a transmembrane region and an N-terminal domain which defines the ligand specificity (Guicciardi & Gores 2009). The cytoplasmic region is known as the death domain (DD) and is crucial for induction of apoptosis. FAS, TNF receptor 1 and TRAIL-R1/R2 (TNF-related apoptosis inducing ligand receptor 1 and 2) are the most known and studied death receptors in the TNF superfamily (Mandal et al. 2020). FAS and TRAIL receptor activations are associated with apoptotic signaling, while TNF receptor also stimulates inflammatory signaling via the NF-κB pathway (Guicciardi & Gores 2009).

Binding of the death ligands FAS-L or TRAIL to their FAS or TRAIL-R receptors, respectively, leads to conformational changes in the receptors, further promoting recruitment and binding of FADD (FAS Associated Death Domain) through individual DD interactions, as illustrated in Figure 2A. Binding of FADD to the death receptor leads to the recruitment of procaspase-8 via a homotypic interaction between the N-terminal DED domains of FADD and procaspase-8. This leads to the formation of DISC (Death-Inducing Signaling Complex) which consists of a death receptor, FADD and procaspase-8 (Mandal et al. 2020). Noteworthy is that a single FADD molecule can bind multiple procaspase-8 molecules, and that the DISC can contain up to 9-fold more procaspase-8 than FADD (Dickens et al. 2012). Dickens et al. (2012) proposed a Chain-Assembly model to describe this finding where the DED of FADD interacts with DED1 of procaspase-8 whose DED2 in turn interacts with DED1 of another procaspase-8, forming a DED chain. Besides the recruitment of procaspase-8 to form the DISC, also the long form of FLICE-like inhibitory protein, $cFLIP_L$, can be recruited to the complex (Guicciardi & Gores 2009). cFLIPs are described in more detail later in Chapter 1.2.4.

Formation of the DISC complex leads to the activation of Caspase-8 by dimerization and two-step autoproteolytic cleavage. Dimerization occurs via homo-oligomerization of two procaspase-8 molecules, or via hetero-oligomerization with the proteolytically dead Caspase-8 homolog, cFLIP (Orning & Lien 2021). Initiator caspases activate downstream effector caspases through their aspartate-specific proteolytic activity. The apical Caspase-8, on the other hand, has little protease activity and is thought to be activated via an induced proximity model (IPM). This model was initially introduced by Salvesen and Dixit in 1999, suggesting that recruitment and clustering of procaspases at the DISC leads to their self-processing. Pop et al. (2007) demonstrated that the autocleavage of

procaspase-8 is not alone sufficient for the catalytic activation of Caspase-8, but that dimerization is required to enhance the cleavage and to stabilize the dimer.

After dimerization, Caspase-8 homodimers are processed through a two-step cleavage (Mandal et al. 2020). The first cleavage occurs between the small and large subunits at Asp374 residue, leading to the formation of subunits p41/43 and p12. The second cleavage occurs between the large subunit and prodomain at the Asp216 and Asp384 residues, cleaving of the p41/43 fragments, and resulting in the generation of subunits p26/24, p18 and p10. Two large and two small subunits, p18 and p10, respectively, form a catalytically active Caspase-8. It appears that the release of the small subunit p10 has two functions, reducing the auto-processing activity of Caspase-8 and similarly increasing the access of Caspase-8 substrates, for example Caspase 3 and 7 as well as BID (Hughes et al. 2009).

Dimerization and cleavage of Caspase-8 lead to the release of Caspase-8 into the cytosol in an active heterotetrameric form. Active Caspase-8 can cleave effector caspases, procaspase-3 and -7, leading to activation of a caspase cascade, resulting in cleavage and degradation of other cellular proteins and eventually apoptosis (Fig. 2A). The downstream signaling of DISC depends on the amount of released active Caspase-8 in the cytosol (Guicciardi & Gores 2009). High levels of Caspase-8 trigger the caspase cascade resulting in apoptosis. Low levels of Caspase-8 in the cytosol can lead to the cleavage of the proapoptotic BID protein which can then translocate into the mitochondria and lead to activation of the intrinsic apoptosis pathway by oligomerization with the Bcl-2 family proteins Bax or Bak.

Activation of the death receptors FAS and TRAIL activate Caspase-8 in a similar manner, whereas the activation of the TNF receptor (TNF-R) mediates apoptosis in a different mechanism (Mandal et al. 2020), as illustrated in Figure 2B. TNF-R is activated by binding of the TNFα ligand to the receptor. Activation of TNF-R leads to recruitment and binding of TRADD (TNF-R Associated Death Domain) to the cytoplasmic tail of TNF-R, which further recruits RIPK1 (receptor-interacting protein kinase 1) through their mutual death domains. Binding of TRADD to TNF-R leads to recruitment of TRAFs (TNF-R-associated factor) and cIAP proteins (cellular inhibitor of apoptosis). cIAPs ubiquitylate RIPK1 leading to the formation of Complex I and the activation of NF-κB and MAPK pathways, resulting in proinflammatory cytokine and chemokine excretion.

RIPK1 is de-ubiquitylated by the CYLD enzyme (Ubiquitin Carboxyl-Terminal Hydrolase) or via inhibition of cIAPs (Declercq et al. 2009). De-ubiquitylation of RIPK1 leads to its dissociation from the Complex I, enabling formation of Complex IIa (ripoptosome) or Complex IIb (necrosome) through RIPK1 interaction with RIPK3. When active Caspase-8 is present in the cytosol as a homodimer, both kinases RIPK1 and RIPK3 are cleaved, leading to release of Caspase-8 from the Complex IIa and resulting in activation of apoptosis by cleaving procaspase-3 (Tsuchiya et al. 2015). However, when active Caspase-8 is formed with $cFLIP_L$, and is present in the cell as a heterodimer, it can cleave RIPK1 but is unable to initiate apoptosis due to its weak protease activity towards effector caspases. If expression of FADD is downregulated or Caspase-8 activity is inhibited by somatic mutations or $cFLIP_s$, Complex IIb is formed (Lee et al. 2012). Resulting from the formation of this complex, Caspase-8 is unable to cleave RIPK1 and RIPK3, leading to activation of these kinases via their mutual phosphorylation. Activation of RIPK3 leads to recruitment and activation of MLKL (mixed-lineage kinase domain-like) which can then translocate to the plasma membrane and initiate necroptosis (Fig. 2B).

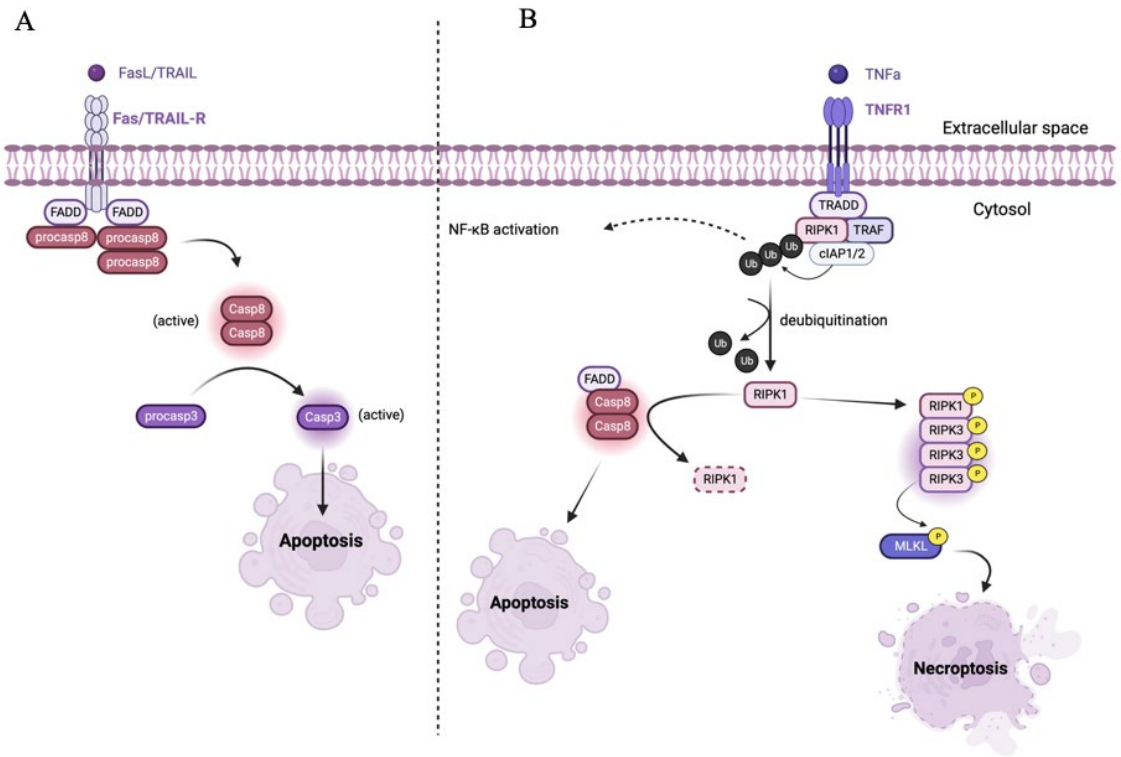

Figure 2. Extrinsic apoptotic signaling mediated by FAS/TRAIL-R and TNF-R. A) FAS/TRAIL-R activation leads to recruitment of adaptor proteins FADD and procaspase-8, leading to formation of DISC. Dimerization and cleavage of the procaspase-8 zymogen activates Caspase-8, which can then activate the caspase cascade by cleaving effector caspases, and finally leading to apoptosis. B) TNF-R activation leads to recruitment of

TRADD, RIPK1, TRAFs and cIAP proteins. Ubiquitylation of RIPK1 leads to activation of the NF-κB signaling pathway, while de-ubiquitylated RIPK1 can interact with FADD and Caspase-8. Caspase-8 cleaves RIPK1, resulting in activation of apoptosis. If Caspase-8/FADD levels are low, Caspase-8 is unable to cleave RIPK3, leading to activation of MLKL and initiation of necroptosis. (Berghe et al. 2014; Henry & Martin 2017; Mandal et al. 2020). Created with BioRender (available at https://www.biorender.com).

1.2.2 Caspase-8 in inflammatory signaling

Caspase-8 has a non-enzymatic role in the NF-κB signaling pathway independent from its catalytic activity (Henry & Martin 2017). The NF-κB pathway regulates innate and adaptive immune responses and induces inflammation through regulating transcription of pro-survival genes, cytokines and chemokines. Caspase-8 can induce upregulation of chemokines and cytokines without processing of the zymogen. Activation of TRAIL receptor recruits FADD and binding of procaspase-8, as described in Chapter 1.2.1. Procaspase-8 acts as a scaffold recruiting RIPK1, leading to formation of FADDosome that consists of TRAIL receptor, FADD, procaspase-8 and RIPK1, as illustrated in Figure 3. Formation of this complex leads to ubiquitylation of RIPK1 and subsequent requirement of IKK complex (IκB kinase) and TAK/TAB complex (transforming growth factor ß-activated kinase & TAK1-binding protein). IKK molecules are then phosphorylated by TAK followed by phosphorylation and degradation of NF-κB inhibitor, IκB. This leads to the activation of NF-κB which can then translocate into the nucleus and induce the expression of cytokine and chemokine genes.

Henry & Martin (2017) demonstrated that catalytically inactive Caspase-8 was resistant to TRAIL-induced cell death, while it did not have any effect on TRAIL-induced inflammatory signaling, suggesting a scaffold-only role for procaspase-8. They confirmed these findings by assessing actions of catalytically inactive Caspase-8 and *CASP8* knockouts. Both knockout and oligomerization-defective mutant of *CASP8* suppressed TRAIL-induced apoptosis and inflammatory signaling. The study therefore suggests that TRAIL-induced cytokine and chemokine production crucially requires oligomerization of procaspase-8 molecules through their DED2-DED2 interactions.

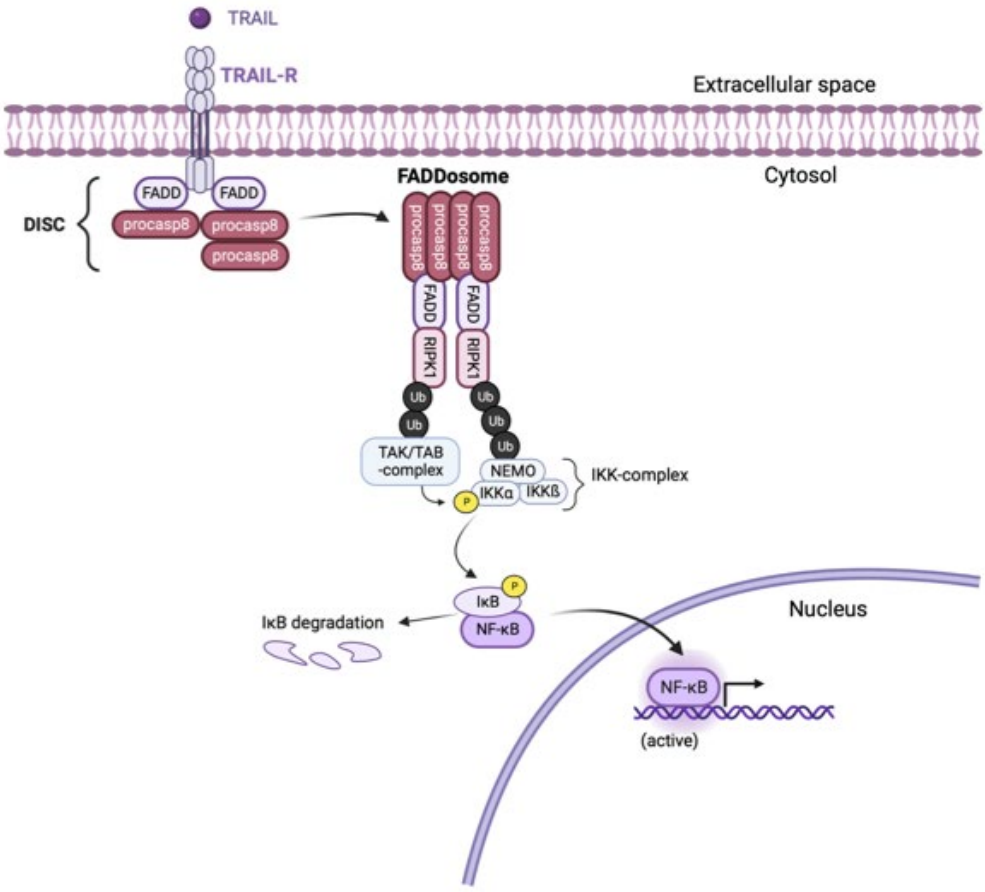

Figure 3. TRAIL-R-mediated NF-κB signaling pathway. Following TRAIL-R activation, procaspase-8 acts as a scaffold for formation of FADDosome, consisting of TRAIL-R, FADD, procaspase-8 and RIPK1. Formation of this complex leads to ubiquitylation of RIPK1 and subsequent requirement of IKK complex. IKK molecules are phosphorylated by TAK followed by phosphorylation and degradation of IκB, leading to activation of NF-κB. NF-κB can then translocate into the nucleus and induce the expression of cytokine and chemokine genes. (Berghe et al. 2014; Henry & Martin 2017; Mandal et al. 2020). Created with BioRender (available at https://www.biorender.com).

1.2.3 Caspase-8 as an inhibitor of necroptosis

Necroptosis refers to regulated necrosis which is a form of cell death that is activated in response to inflammation, bacterial or viral infections, resulting in cellular rupture and leakage. Necroptosis widely differs from apoptosis, one remarkable difference being that Caspase-8 acts as an inhibitor of necroptosis (Tummers & Green 2017). Extrinsic apoptosis depends on the activation of initiator and effector caspases, whereas necroptosis depends on the kinase activity of RIPK1 and RIPK3 to activate MLKL. Caspase-8 inhibits necroptosis mainly by cleaving RIPK1 but also RIPK3 and CYLD (Berghe et al. 2014) (Fig. 2B).

Necroptosis is induced by TNFR1 ligation. Binding of de-ubiquitylated RIPK1 and RIPK3 leads to oligomerization of RIPK3 and further activation and binding of effector protein MLKL. This effector protein then translocates to the plasma membrane and induces rupture and cellular leaking, resulting in cell death (Berghe et al. 2014; Tummers & Green 2017). Tummers and Green (2017) reviewed that necroptosis occurs if cells are lacking FADD or Caspase-8, indicating the role of the DISC complex in regulating necroptosis. Inhibition of Caspase-8 resulted in inhibition of RIPK1 and RIPK3 cleavage, leading to TNF-induced RIPK3 activation and necroptosis, indicating the regulatory role of Caspase-8 in inhibiting necroptosis. Caspase-8 can therefore regulate the balance between apoptosis and necroptosis in cells.

1.2.4 Regulators of Caspase-8 activity

Activity of Caspase-8 can be regulated and affected by various mechanisms. As mentioned previously (Chapter 1.2.1), the amount of released active Caspase-8 in the cytosol can determine whether a cell progresses to activation of caspase cascades or to intrinsic apoptotic signaling by cleaving BID (Guicciardi & Gores 2009). In addition, the ubiquitylation of RIPK1 regulates the destiny of cells, determining whether cells survive or go through apoptosis after TNF receptor activation (Tummers & Green 2017). Yet, major regulators of Caspase-8 activity are the FLICE-like inhibitory proteins, $cFLIP_L$ and $cFLIP_S$.

cFLIP regulates Caspase-8 driven apoptosis and determines whether a cell dies by binding to the DISC complex (Tummers & Green 2017). cFLIP is a Caspase-8 homolog that does not have any catalytic activity. Depending on the post-transcriptional mRNA splicing, two isoforms of cFLIP can be formed, cFLIP long ($cFLIP_L$) and cFLIP short ($cFLIP_S$) (Irmler et al. 1997). The latter has only two DED domains and a short C-terminal tail, being a truncated form of procaspase-8. $cFLIP_L$, on the other hand, resembles full-size procaspase-8 but is proteolytically dead due to absence of a catalytic cysteine in the large subunit.

$cFLIP_S$ inhibits Caspase-8 activation by forming heterodimers with procaspase-8 and by disrupting the formation of DED-dependent procaspase-8 chain in the DISC (Tsuchiya et al. 2015). In contrast, the function of $cFLIP_L$ is more diverse and complex, since low levels of the protein enhance the extrinsic apoptotic signaling, while high levels inhibit

apoptosis (Chang et al. 2002). $cFLIP_L$ is recruited to the DISC complex by procaspase-8. Heterodimerization of procaspase-8 with $cFLIP_L$ rearranges the catalytic site of procaspase-8 and activates the heterodimer without proteolytic processing, leading to limited substrate specificity (Hughes et al. 2016). Thus, high levels of $cFLIP_L$ can regulate procaspase-8 activation by inhibiting the formation of procaspase-8 filaments (Tummers & Green 2017). Low expression levels of $cFLIP_L$ lead to formation of highly active heterodimers with procaspase-8, resulting in increased apoptotic signaling (Hughes et al. 2016). Therefore, $cFLIP_L$ has a dual role as both a positive and a negative regulator of activation of Caspase-8. In addition to the above-mentioned regulatory role of cFLIP, it can also control the formation of Complex IIa (ripoptosome) and is most likely involved in necroptosis (Tsuchiya et al. 2015). Hence, the different isoforms and expression levels of cFLIP are crucial determinants for Caspase-8 activity and the fate of the cell.

1.3 *CASP8* mutations in cancer

The hallmarks of cancer include avoiding growth suppressors and immune destruction, replicative immortality, activation of metastasis and invasion, genome instability, ability to induce vascularization and deregulating cellular metabolism (Hanahan 2022). Tumor-promoting inflammation and ability to resist and avoid cell death are also deceptive characters of cancer cells. Caspase-8 impairment is one main way to disturb apoptosis, and mutations in *CASP8* might enhance proliferation and migration of cancer cells (Lowe & Lin 2000). The cBioPortal database contains 10 967 samples from TCGA studies of which 3 % have *CASP8* mutations (Cerami et al. 2012; Gao et al. 2013). *CASP8* mutation frequency is the highest in HNSCC, it is mutated in 10,7 % of cancer cases (Figure 4). Mutations have been observed also in endometrial and cervical cancers as well as in bladder and esophagogastric cancers, albeit relative rarely.

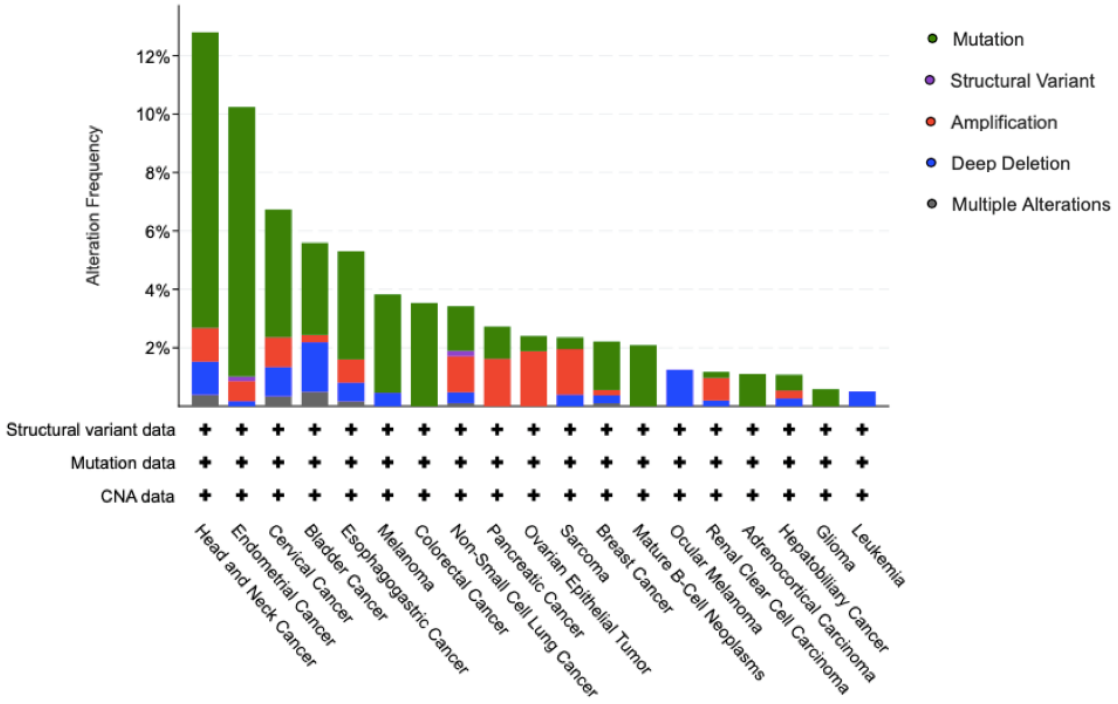

Figure 4. *CASP8* mutation frequency in cancer. *CASP8* is altered in many cancer types but most commonly it is mutated in HNSCC (10,7 %). Alterations of *CASP8* gene include mutations, structural variants, amplifications and deep deletions. Retrieved from cBioPortal, TCGA & PanCancer Atlas 03/2023 (Cerami et al. 2012, Gao et al. 2013).

The long-term perception that Caspase-8 expression would be completely lost in cancer, and therefore affecting the apoptotic signaling negatively, has been overturned. The role of *CASP8* modulations in cancer are rather more complex. Caspase-8 expression is usually normal or even elevated in many cancer cases, while the apoptotic activity is regulated and altered through different mechanisms (Mandal et al. 2020). Studies based on the Human Protein Atlas resource confirm the findings about upregulation of Caspase-8 activity in many epithelial malignancies, such as pancreatic and cervical cancers (Stupack 2013). On the contrary, the same study showed that Caspase-8 expression has been detected to be decreased in prostate cancer. Full deletions of *CASP8* and mutations that fully inactivate the gene are rarely observed in epithelial-derived cancers (Stupack 2013). Even though, inactivating mutations have been detected in gastric cancer (Soung et al. 2005) and homo- or heterozygous deletions of *CASP8* have been observed in neuroblastoma (Teitz et al. 2000), these alterations occur relatively rarely.

Expression of Caspase-8 in malignancies can be affected by oncogenic activities of the developing carcinoma by expressing Caspase-8 inhibitors, activating growth factor

receptors or tyrosine kinases, such as Src, that can inhibit the expression of caspases (Stupack 2013). In addition to the aforementioned, expression of Caspase-8 can be altered by genetic mutations or epigenetic mechanisms, alternative splicing and by posttranslational modifications (Fulda 2009). Hypermethylation has been commonly detected to be the cause of alterations in Caspase-8 functionality in many cancers, including neuroblastoma, glioblastoma or lung cancer (Fulda 2009). Noteworthy is that the location where the methylation usually occurs lack the promoter activity and the CpG islands, which are common sites for methylation (Teng et al. 2017). Furthermore, allelic imbalance of chromosome 2q can lead to alterations in CASP8 expression, which has been observed in neuroblastoma (Takita et al. 2001) and in head and neck cancer, correlating with poor prognosis (Ransom et al. 1998).

Many mechanisms can impair and affect the expression of Caspase-8, which can further promote tumor formation, progression and resistance to cancer treatments (Fulda 2009). As it is noticeable from the aforementioned cancer cases, the alterations in *CASP8* seem not to follow any specific logic as the expression can be downregulated, upregulated or normal in some cancers (Mandal et al. 2020). However, it has been observed that mutations in *CASP8* behave in a dominant-negative manner meaning that one allele mutation is enough to express the mutation phenotype (Li et al. 2014; Cui et al. 2021).

1.3.1 *CASP8* mutations in HNSCC

As mentioned earlier, *CASP8* mutations occur most commonly in HNSCC, with a mutation frequency of 10,7%. Mutations have been found all over the protein coding sequence without any significant hotspots (Leonard & Johnson 2018). The mutation type varies widely among tumors and HNSCC cell lines, since mutations can occur as nonsense, missense, frame-shift or at the splice-site, however suggesting that most of the mutations are loss-of-function (Pickering et al. 2013). The expression level of Caspase-8 is usually normal in HNSCC cases, while its function is altered due to the mutations (Mandal et al. 2020; Cui et al. 2021). *CASP8* mutations have a dual role in development and progression of HNSCC; mutations have been shown to impair and inhibit death receptor-mediated cell death, as well as to promote activation of the NF-κB signaling pathway (Ando et al. 2013; Li et al. 2014; Cui et al. 2021). Moreover, *CASP8* mutations

have been shown to contribute in tumor growth, migration and invasion of cancer cells (Kemmer et al. 2018).

Genomic analysis study by Pickering et al. (2013) revealed that reduced expression of Caspase-8 in HN4 cell lines (human carcinoma cell line derived from HNSCC) resulted in larger and more aggressive tumors. Based on the genomic analysis study, all *CASP8* mutations found in OSCC (Oral squamous cell carcinoma) patients were heterozygous, and mutations were more tumorigenic causing more lethal and larger tumors. Downregulation of *CASP8* has been associated with poorly differentiated tumors, whereas upregulation of the gene in HNSCC patients with lymph node metastasis is remarkably correlated with poor overall survival (Elrod et al. 2010). Furthermore, loss of Caspase-8 function can shift the cell death signaling from apoptosis to necroptosis (see Chapter 1.2.3). However, effect of *CASP8* mutations in the necroptotic signaling and whether the switch affects development of HNSCC remain obscure, since fully inactivating mutations are rarely observed (Stupack 2013; Leonard & Johnson 2018).

HNSCC tumors containing *CASP8* mutations show weak response to such cancer therapies that are based on death receptor-induced cell death (Li et al. 2014). In addition, *CASP8* mutations have been shown to impair the effects of cancer therapies (Figure 1), and mutations correlate negatively with the overall survival of HNSCC patients (Singh et al. 2020; Uzunparmak et al. 2020). Moreover, somatic alteration in *CASP8*, such as gene deletions and hypermethylation, are associated with cytotoxic drug resistance in oral cancers (Usman et al. 2021). Currently, relatively little is known about predictive markers in HNSCC (Li et al. 2014), thus the effect of *CASP8* mutations in cancer therapy responses should be studied.

1.3.2 *CASP8* mutations and resistance to death receptor-mediated cell death

Mutations in *CASP8* can prevent the normal functions of extrinsic apoptosis and death receptor-mediated cell death. Indeed, alterations in these gene have been shown to impair the effect of radiotherapy in HNSCC patients (Fig 1.). *CASP8* mutations observed in HNSCC patients are assumed to be loss-of-function, although their functional properties and phenotypic effects are still poorly understood (Pickering et al. 2013). Li et al. (2014) studied four HNSCC associated *CASP8* mutations, and how they affect the activation of extrinsic apoptotic signaling in addition to cellular migration, invasion and in vivo tumor

growth. Later, also Cui et al. (2021) studied 18 *CASP8* mutations found in HNSCC patients, and their properties in death receptor-mediated cell death as well as effects on the inflammatory response.

Nonsense and missense mutations E89*, L105H, S375* and S386* in *CASP8* showed to inhibit Caspase-8 activation and execution of apoptosis after treatment with TRAIL or anti-Fas antibody (Li et al. 2014). Results from Li et al. suggest that all these four *CASP8* mutations would inhibit the processing of the zymogen (procaspase-8) after death receptor stimulation. As comparison, WT Caspase-8 levels were significantly reduced after TRAIL treatment, indicating the processing of the zymogen after death receptor activation. Thus, mutations in *CASP8* could inhibit the extrinsic apoptotic signaling and execution of apoptosis after death receptor stimulation by possessing resistance to TRAIL treatment.

Cui et al. (2021) showed that *CASP8* mutations L7V, G11E, G11R, S99F and Y178del caused remarkable dose-dependent cell growth inhibition after being treated with TRAIL for 48h, while rest of the mutations were resistant to the death receptor-mediated cell death. It is to be noted that none of the 18 *CASP8* mutations inhibited cell growth after 12h treatment with TRAIL, whereas the WT Caspase-8 reacted to this treatment with dose-dependent cell growth inhibition. Thus, the study showed that 5/8 mutations in the N-terminal prodomain preserved the ability to induce apoptosis after death receptor stimulation, whereas all ten C-terminal catalytic domain mutations were resistant to TRAIL mediated apoptosis. All these C-terminal mutations also retained the capacity to dimerize with WT Caspase-8, while prodomain mutations L7V, G11R, L62P, R71T, S99F and L105H failed in that action.

Findings from Cui et al. (2021) revealed an inverse relationship in HNSCC-associated *CASP8* mutations between their ability to induce dimerization with WT Caspase-8 and to mediate apoptosis after death receptor stimulation by TRAIL. This further indicates more diverse functional properties and phenotypic effects of *CASP8* mutations, rather than only being loss-of-function. All in all, both studies from Li et al. (2014) and Cui et al. (2021) indicate that some of the *CASP8* mutations observed in HNSCC patients could indeed inhibit the activation of apoptotic signaling and cellular death after death receptor stimulation. Therefore, the possibility to utilize the *CASP8* mutations as predictive markers for cancer therapies that are based on death receptor signaling in HNSCC could be discussed.

1.3.3 *CASP8* mutations in NF-κB signaling

The NF-κB signaling pathway is involved in innate and adaptive immune responses, inflammation, cell proliferation and differentiation in addition to apoptosis (Baud & Karin 2009; Xia et al. 2018). Increased NF-κB signaling, and continuous activation of the pathway are associated with many malignancies including breast cancer (Sau et al. 2016), glioblastoma (Zanotto-Filho et al. 2017) and cervical cancer (Li et al. 2009). Increased activation of NF-κB can enhance metastasis, abnormal proliferation and differentiation of cancer cells, as well as treatment resistance and can affect the immune composition of tumor microenvironment (TME) (Xia et al. 2018; Cui et al. 2021). Since Caspase-8 has been shown to play a scaffolding role in the NF-κB signaling pathway (Henry & Martin 2017), mutations in the gene could interfere the normal inflammatory signaling.

Ando et al. (2013) studied 16 *CASP8* mutations, 15 of them have been previously identified form epithelial tumors and one missense mutation (G325A) was discovered in HNSCC cell line. They showed that this novel HNSCC-associated *CASP8* mutation activated the NF-κB pathway to greater extent than WT *CASP8*. Similarly, 12/15 of the previously identified cancer-associated *CASP8* alterations were able to enhance the NF-κB signaling. Only three mutations failed to activate the signaling pathway, and those were all located in DED1 or DED2 in the prodomain of Caspase-8. Moreover, mutations in the catalytic domain of Caspase-8 were shown to negatively affect the processing ability of the zymogen. However, Cui et al. (2021) demonstrated the retained capacity of catalytic domain mutations to dimerize with wild-type Caspase-8.

Caspase-8 mediates the inflammation signaling and secretion of cytokines and chemokines via NF-κB pathway. Cui et al. (2021) studied the functional properties of 18 HNSCC-associated *CASP8* mutations and how they affect the production of cytokines and chemokines (IL-6, IL-8 and CXCL1) in cancer cells. They showed that 5/8 prodomain mutations and only 1/10 catalytic domain mutation failed to induce the NF-κB pathway-mediated induction of IL-6, IL-8 or CXCL1 after death receptor activation by TRAIL. As expected, *CASP8* knockout cells failed to activate the NF-κB pathway after death receptor activation. Mutations L62P, Y178del, D303G, D308G, and S375* were able to upregulate production of all three cytokines and chemokines in a dose-dependent fashion and even greater than twofold after death receptor stimulation. Most of the studied *CASP8* mutations retained the ability to activate the NF-κB signaling after TRAIL treatment,

which further confirmed the diverse functional properties of HNSCC-associated *CASP8* mutations. *CASP8* mutations could have gain-of-function properties in inflammatory signaling, rather than loss-of-function, (Ando et al. 2013) leading to enhanced secretion of cytokines and chemokines, which further can promote the TME into more favorable milieu for cancer cells (Cui et al. 2021). In vivo studies by Cui et al. (2021) showed that the catalytic domain mutation D303G could indeed impact the immune composition of tumor.

Taken together, studies by Ando et al. (2013) and Cui et al. (2021) showed that mutations in the catalytic domain of Caspase-8 were more likely to retain the ability to activate the NF-κB signaling, whereas mutations in DED1 and DED2 were prone to affect the inflammatory signaling negatively. Therefore, the DED domains of Caspase-8 might play significant roles in the activation of NF-κB signaling, and mutations in the prodomain might affect the scaffold formation.

1.4 Aims of the study

As mentioned earlier, *CASP8* mutations can impair the apoptotic signaling mediated by death receptors. In addition, *CASP8* mutations can enhance the secretion of cytokines and chemokines after death receptor activation and thus could have an impact on the TME. *CASP8* mutations might correlate with poor survival prognosis of HNSCC patients when being treated only with radiation, as illustrated in Figure 1. Therefore, it is of high importance to identify the mechanisms in cancer cells that are associated with cancer therapy resistance. Relatively little is known about markers in HNSCC to predict the outcome of cancer therapies. Results from this study could be exploited into HNSCC patient samples and could be evaluated whether some of these *CASP8* mutations could act as predictive markers in HNSCC.

CASP8 mutations in this thesis work were selected according to Cui et al. (2021). Nine HNSCC-associated mutations L7V, L62P, R71T, S99F, L105H, D303G, S375*, T441I, Q465* were studied, of which five are located in the prodomain of Caspase-8 and four in the catalytic domain (Fig. 5). S375* and Q465* are nonsense mutations and the remaining seven are missense mutations. HeLa cells were used in this thesis work because the effects of *CASP8* mutations on the function of Caspase-8 are known in HeLa cells and previously studied (Cui et al. 2021). Moreover, HeLa cells are shown to be sensitive to TRAIL-

induced Caspase-8 dependent apoptosis and cytokine induction (Henry & Martin 2017; Cui et al. 2021). Furthermore, by using HeLa cells, as opposed to different cancer cells harboring endogenous *CASP8* mutations, the impact of genetic/phenotypic heterogeneity could be minimized. In this study, the endogenous *CASP8* was knocked out from HeLa cells in order to study homozygous mutations.

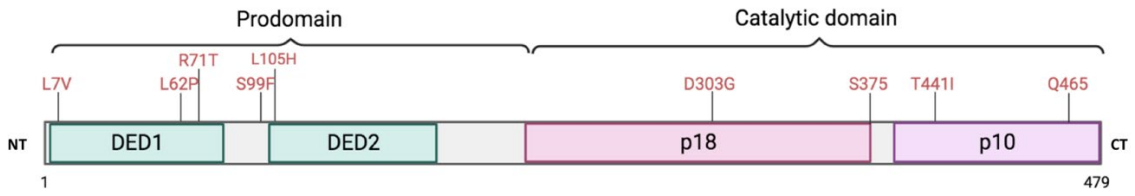

Figure 5. The protein structure of procaspase-8 and nine HNSCC-associated *CASP8* mutations that are studied in this thesis. Mutations with amino acid numbers are indicated on red at the top and they are marked to scale. Procaspase-8 consists of two DED domains in the prodomain and of large and small subunits, p18 and p10, respectively, in the catalytic domain. NT= N-terminus, CT= C-terminus. Created with BioRender (available at https://www.biorender.com)

The first aim of this thesis was to determine whether HNSCC-associated *CASP8* mutations confer resistance to radiation. Based on the previous studies by Li et al. (2014) and Cui et al. (2021), hypothesis was that some of these *CASP8* mutations could impair the response of radiation in cancer cells. The second aim was to determine whether *CASP8* mutations affect the inflammation signaling through NF-κB pathway when induced by radiation and TRAIL. Based on the previous result (Ando et al. 2013; Cui et al. 2021), hypothesis was that mutations in the catalytic domain of Caspase-8 could enhance the NF-κB signaling, and thereby secretion of cytokines and chemokines, whereas mutations in the prodomain could impair the inflammation signaling.

2 Material and methods

2.1 Cell lines and cell culture

HeLa cells and HEK293T cells were used in this thesis work. Both cell lines were stored at -150°C in freezing media containing 8 % of Fetal Bovine Serum (FBS, S181B-500, Biowest) in Dimethyl Sulfoxide (DMSO, BP231-100, Fisher bioreagents). HeLa cells were used in this thesis project because effect of *CASP8* mutations on the CASP8 functionality is known and previously studied (Cui et al. 2021). HEK293T cells were utilized in lentiviral transduction.

Cells were cultured in Dulbecco's Modified Eagle's Medium, DMEM, (ECM0728L, EuroClone) supplemented with heat-inactivated 10 % FBS and 1 % penicillin/streptomycin (ECB3001D, EuroClone). Created HeLa *CASP8* mutation cell lines (HeLa CASP8-MT/WT) were cultured in same conditions as WT HeLa cells but supplemented also with 1 µg/ml puromycin (A11138-03, Gibco) as a selection antibiotic. Cells were cultured in standard cell culture conditions at +37°C with 5 % CO_2.

2.2 Creation and characterization of HeLa *CASP8* knock-out cells

Prior to this thesis work, HeLa cells were subjected to CRISPR/CAS9 genome editing to create *CASP8* knock-out cells using previously described methodology (Kurppa et al. 2020). Here, the bulk population of edited cells were single-cell cloned and the clones were screened for absence of CASP8 protein using western blot. Successful HeLa *CASP8* knock-out clones (HeLa$^{CASP8-/-}$) were chosen for subsequent experiments.

2.2.1 Western blotting

Cells were lysed with lysis buffer and collected from 6-well plates. Lysates were incubated on ice for 15 mins followed by centrifugation (11 000g) at +4°C for 15 min. Protein concentrations were measured from supernatants with Protein Assay Dye Reagent Concentrate 5x (5000006, Bio-Rad) and absorbances were analysed with Multiskan FC (Thermo Scientific). Equal amounts of protein (15 µg/µl) from each sample were prepared with 6 x SDS-SB (final SDS-SB 1x), denatured at +95°C for 5 min and separated

on a self-made 10 % Tris-Glycine gel. Proteins were transferred overnight to a Cellulose Nitrate Strips (11327 41BL, Sartorius) followed by blocking with 5 % milk-TBST for 1h at room temperature (RT), and overnight incubation with primary antibodies Caspase-8 (D35G2, Cell signaling technology) and anti-GAPDH (5G4CC, Sigma-Aldrich). GAPDH, a housekeeping protein, was blotted to ensure that equal amounts of protein were loaded on the gel from each sample.

Membranes were washed 3 x 5 min with TBST, and secondary antibodies (Goat anti-rabbit 926-68071, Donkey anti-Mouse 926-68072, Li-Cor) were incubated for 1h at RT, protected from light. After antibody binding, membranes were again washed with TBST and protein expressions were detected with Odyssey CLx imaging system (Li-Cor Biosciences).

2.2.2 Irradiation experiments

Irradiation and proliferation assays were performed to characterize the features and properties of HeLa$^{CASP8-/-}$ cell lines, in relation to WT HeLa, in order to select the most suitable cell line for further experiments. HeLa$^{CASP8-/-}$ cells (clones #7, #18, #21, #35, #38 and #41) as well as WT HeLa were plated at the same time for irradiation and proliferation assays; 1000 cells /well on 96-well plates with six replicates from each cell line. Cells were irradiated with Faxitron MultiRad350 (Precision) with doses of 0, 2, 4, 6 and 8 GY (320kV, 12 mA). Cell viabilities were measured with MTT assay (MTT Dye Solution G4102, Promega, and STOP solution containing 0,6 % Acetic acid, 10 % SDS in DMSO) 7 days after irradiation. Absorbances were measured with Cytation 5 AH diagnostic (BioTek) using program Gen5 Image Prime 3.08 and irradiation sensitivities were analysed with Prism GraphPad (Dotmatics, available at https://www.graphpad.com).

2.2.3 Proliferation experiments

To determine the proliferation of HeLa$^{CASP8-/-}$ in relation to WT HeLa, MTT assays were performed on days 1, 3, 5 and 7 from plating. Absorbances were measured with Cytation 5 AH diagnostics (BioTek) with program Gen5 Image Prime 3.08 and results were analysed with Prism GraphPad (Dotmatics, available at https://www.graphpad.com).

2.3 Generation of lentiviral expression vectors encoding wild-type and mutant *CASP8*

2.3.1 Inserting a Flag-tag to *CASP8* cDNA

Prior to cloning of *CASP8* mutations to plasmids pDONR221-*CASP8*, a flag-tag was cloned to the C-terminus of *CASP8* in this plasmid with PCR using Phusion® Hot Start Flex 2X Master Mix (M0536S, NEB). 10 ng of plasmid DNA (pDONR221-*CASP8*) and 0,5 µM of primers KJK239 and KJK240 (see Appendix 1) were used in total volume of 50 µl/ reaction. PCR cycling conditions were as following: initial denaturation at +98°C for 30 s, 35 cycles of +98°C 30 s, +60°C 20 s, +72°C 1 min 20 s, and final extension at +72°C for 5 min. PCR fragments were separated on a 1 % agarose gel and correct replicates were chosen to be continued with. After this, methylated plasmid DNA templates were degraded from the PCR product with 1 ul of DpnI (FD1703, Thermo Fisher Scientific). Reactions were incubated for 1 h at +37°C, followed by purification of the PCR reactions with NucleoSpin® Gel and PCR Clean-up kit (740609.250 Macherey-Nagel) according to the protocol. Purified PCR reactions (100 ng) were re-ligated with Quick Ligase (M2200S, NEB) in total reaction volume of 21 µl and incubated for 15 mins at RT.

pDONR221-*CASP8*-Flag plasmids were propagated in competent *E. coli* Dh5α cells. Bacteria were transformed with 5 µl of ligation reaction per 40 µl of Dh5α and incubated on ice for 30 min, followed by heat shock at +42°C for 45 s. Reactions were incubated with LB medium (LB Broth (Lennox) (H26760, Alfa Aesar), diluted in MQH_2O) at +37°C rocker for 1 h, after which LB was decanted out and bacteria plated into LB + kanamycin plates. Plates were let to grow overnight at +37°C and six individual colonies were selected for further growth in 5 ml LB-medium with 1:1000 kanamycin added. After overnight growth at +37°C minipreps were made using NucleoSpin® Plasmid kit (740588.250, Macherey-Nagel), according to protocol. Plasmids were digested with EcoRI (FD0274, Thermo Scientific) and EcoRV (FD0304, Thermo Scientific) to pre-screen for correct plasmid size. Finally, insertion of flag-tag to pDONR221-*CASP8* was ensured with Sanger sequencing (Eurofins Genomics) and results were analysed with SnapGene (Dotmatics, available at https://www.snapgene.com)

2.3.2 Cloning of *CASP8* mutations to pDONR221-*CASP8*-flag

Nine *CASP8* mutations (L7V, L62P, R71T, S99F, L105H, D303G, S375*, T441I, Q465*) were generated into the pDONR221-*CASP8*-Flag plasmid. The site-directed mutagenesis was carried out using PCR in a reaction containing Phusion Green 5x HF buffer, dNTP (0,2 µM), 3 % DMSO, 1 U Velocity DNA Polymerase (BIO-21099, Bioline), 1 U Phusion DNA Polymerase (F530L, Thermo Fischer Scientific), mutation specific primers (0,5 µM) and plasmid DNA pDONR221-*CASP8*-Flag (10 ng) in total reaction volume of 50 µl. Mutation primers are listed in Appendix 1. PCR cycling conditions were as following: +98°C 30 s, 35 cycles of +98°C 10 s, +61°C 20 s, +72°C 1 min 20 s, and final extension at +72°C for 5 min. Success of PCR was ensured by separating PCR fragments on a 1 % agarose gel. DpnI digestion, purification, re-ligation, transformation, minipreps and restriction digestion pre-screen of the mutant pDONR221-*CASP8*-MT-Flag plasmids were performed as above (Chapter 2.3.1). Successful mutagenesis was ensured with Sanger sequencing (Eurofins Genomics) and results were analysed with SnapGene (Dotmatics, available at https://www.snapgene.com).

2.3.3 Generating doxycycline-inducible lentiviral expression vectors encoding *CASP8* mutations

Plasmids containing *CASP8* mutations (pDONR221-*CASP8*-MTs-Flag) and WT *CASP8* (pDONR221-*CASP8*-Flag) were cloned to destination vector pCW57.1 (Addgene #41393) using Gateway LR cloning. This destination vector pCW57.1 enabled doxycycline-induced gene expression in HeLa CASP8-MT/WT cell lines. Each LR reaction contained 50 fmol of both plasmids pDONR221-*CASP8*-MTs-Flag or pDONR221-*CASP8*-Flag (142 ng) and pCW57.1 (290 ng), LR Clonase™ II enzyme mix (11791-020, Invitrogen) and TE buffer (pH 8.0). All ten reactions were incubated at RT for 2 h followed by incubation at +37°C for 10 mins with Proteinase K (Invitrogen) to terminate LR reactions.

Competent *E. coli* Dh5α were transformed with 5 µl of LR reactions (nine *CASP8* MTs and WT *CASP8*) per 50 µl of bacteria. Incubation, heat shock, LB culture and minipreps were performed as above (Chapter 2.3.1), the only difference being that carbenicillin

(1:1000) was used on Agar plates and in LB culture. pCW57.1-*CASP8*-MTs-Flag and pCW57.1-*CASP8*-Flag plasmids were digested with either FastDigest CSiI (FD2114, Thermo Fisher Scientific) or XhoI (R0146S, NEB) to pre-screen for correct plasmid size prior sequencing (Eurofins Genomics). Results were analyzed with SnapGene (Dotmatics, available at https://www.snapgene.com).

2.3.4 Transient transfection of HeLa$^{CASP8-/-}$ cells

In order to select the most suitable HeLa$^{CASP8-/-}$ cell line from single cell cloning (see Chapter 2.2) to create stable mutation cell lines, HeLa$^{CASP8-/-}$ cell lines (clone #21 and #38) were transiently transfected with pBABE-*CASP8*-Flag and pBABEpuro-eGFP. pBABE-*CASP8*-Flag plasmid was constructed as described above in Chapter 2.3.3, only difference being that destination vector was pBABE-puro-gateway plasmid instead of pCW57.1.

HeLa$^{CASP8-/-}$ cells (clone #21 ad #38) were plated on 6-well plate 3x10^5 cells /well. Cells were transfected with pBABE-*CASP8*-Flag or pBABEpuro-eGFP using FuGENE® 6 Transfection reagent (E2691, Promega). After 6 h incubation at +37°C transfected cells and WT HeLa cells were plated on 96-well plate 2000 cells /well for MTT assay. MTT assays were performed as above (Chapter 2.2.2) on days 1, 3 and 5 after transfection to determine the proliferation of cells.

Rest of the transfected cells and WT HeLa cells were plated on a 6-well plate. GFP signals were observed with EVOS M5000 Microscope (Thermo Fisher Scientific) to ensure successful transfection, after which cells were lysed and western blot was performed as described in Chapter 2.2.1. Protein expressions were visualized with Odyssey CLx imaging system (Li-Cor Biosciences).

2.4 Generation of stable HeLa CASP8-MT/WT cell lines

HeLa$^{CASP8-/-}$ clone (#21) was virally transduced with pCW57.1-*CASP8*-MTs-Flag plasmids that contained nine *CASP8* mutations (L7V, L62P, R71T, S99F, L105H, D303G, S375*, T441I, Q465*), and WT *CASP8* (pCW57.1-*CASP8*-Flag, later marked as

CASP8-WT) to act as a control. Creation of stable HeLa cell lines expressing *CASP8* mutations and WT *CASP8* was carried out using 3rd generation lentiviral transduction.

HEK293T cells were plated 4 x 10^5 cells on a T25 flask and transfected with lentiviral packaging plasmids pMDLg/pRRE (1 µg, Addgene #12251), pMD2.G (500 ng, Addgene #12259), pRSV-Rev (500 ng, Addgene #12253) and 2 µg of expression plasmids pCW57.1-*CASP8*-L7V/L62P/R71T/S99F/L105H/D303G/S375*/T441I/Q465*/WT using FuGENE® 6 Transfection reagent (E2691, Promega). Transfected HEK293T cells were taken immediately to the BSL2 virus laboratory. Medium was changed to fresh culture media (DMEM) 6h after transfection.

HeLa$^{CASP8-/-}$ (clone #21) cells were plated at a density of 1,8 x 10^5 cells on T25 flasks (one flask for each *CASP8* mutation and WT *CASP8*). Viral media from HEK293T cells were collected after 2 days from transfection, filtered and applied to HeLa$^{CASP8-/-}$ cells, with polybrene (10 µg/ml) added. After 2 days, viral media was replaced with fresh medium (DMEM) supplemented with puromycin (2 µg/ml). Cells were cultured in the virus laboratory until antibiotic control cells were dead and few passages were done. Absence of replication-competent lentiviruses (RCV) in transduced cells was tested by QPCR, using QuantStudio™ 3 Real-Time PCR system (Thermo Fisher Scientific) with PowerUp™ SYBR™ Green Master Mix (A257/42, Thermo Fisher Scientific) with primers fw/rev-LV-RRE (see Appendix 1). Following negative RCV test, the cells were brought out from the BSL2 virus laboratory to regular BSL1 cell culture. 1 µg/ml of selection antibiotic puromycin (A11138-03, Gibco) was used in cell culture of created HeLa CASP8-MT/WT cells, but not in experiments.

2.4.1 Doxycycline titration

Characterization of created HeLa CASP8-MT/WT cell lines was carried out using doxycycline titration and CASP8 protein detection. Cells were plated on 96-well plates 3000 cells /well as triplicates. Doxycycline Hyclate (324385-1GM, Merck) was added to cells with HP digital dispenser (0,3 % Tween added) as 1:2 titration in concentrations of 3,9–1000 ng/ml. After 72 h MTT assay was performed as above (Chapter 2.2.2). Absorbances were measured with Cytation 5 AH diagnostics (BioTek) and program Gen5 Image Prime 3.08, after which results were analyzed with Prism GraphPad (Dotmatics, available at https://www.graphpad.com). This experiment was repeated multiple times.

2.4.2 Western blotting

In order to confirm correct functionality of doxycycline-inducible CASP8 expressions in HeLa CASP8-WT cells, doxycycline titration was performed after which protein expressions were detected by western blot. HeLa CASP8-WT and WT HeLa cells were plated at 2 x 10^5 amount of cells /well on 6-well plates. HeLa CASP8-WT cells were treated with Doxycycline Hyclate (324385-1GM, Merck) in concentrations of 3,9–1000 ng/ml (1:2 titration), whereas WT HeLa cells were left untreated. Cells were lysed after 24 h and also dead cells from suspension were harvested. Protein samples (30 µg) and western blot experiment were performed exactly as described in Chapter 2.2.1. In addition, expression of PARP and β-tubulin were detected with antibodies PARP (46D11, Cell Signaling technology) and β-tubulin (T7816, Sigma).

Doxycycline-induced CASP8 expressions were also characterized with all HeLa CASP8-MT cell lines (L7V, L62P, R71T, S99F, L105H, D303G, S375*, T441I, Q465*) and HeLa CASP8-WT. HeLa CASP8-MT/WT cells were plated on 6-well plates 1,5 x 10^5 cells /well as replicates. From each cell line the other replicate was left untreated and the other was treated with doxycycline (264 ng/ml). This doxycycline concentration was based on IC50-values from previously conducted titration assays. Cells were lysed after 24 h, after which protein samples (15 µg) and western blot assay were conducted as described in Chapter 2.2.1, the only difference being that proteins were resolved on a commercial Criterion™ TGX™ Precast Gels (5671085, Bio-Rad). Presence and absence of CASP8 in -/+ doxycycline treated cells were detected with Caspase-8 (ab32397, Abcam) primary antibody and after secondary antibody incubation, protein expressions were analyzed with Odyssey CLx imaging system (Li-Cor Biosciences).

2.4.3 Irradiation experiments

HeLa CASP8-MT/WT cells were plated at amount of 1000 cells /well on 96-well plates, five replicates from each cell line. Cells were treated with 30 ng/ml of Doxycycline Hyclate (324385-1GM, Merck) 24 h prior irradiation. HeLa CASP8-WT cells had five replicates treated with doxycycline and five were left untreated. Irradiation was performed as above (Chapter 2.2.2) following with MTT assay five and six days after irradiation. Irradiation experiment was repeated three times with similar conditions, only

two first replicates were five-day experiments and in the third replicate viability was measured six days after irradiation.

2.5 Quantitative PCR

2.5.1 RNA extraction

The effects of *CASP8* mutations to cytokine expression induced by irradiation and human recombinant TRAIL were studied. HeLa CASP8-MT/WT cells were plated 6 x 10^4 cells /well on 6-well plates, one replicate from each MT cell line and two replicates from WT cell line. Cells were treated with 30 ng/ml of Doxycycline Hyclate (324385-1GM, Merck) and one replicate of WT cells was left untreated. After 24 h cells were irradiated with Faxitron MultiRad350 (Precision) with doses of 0 or 8 GY. 24 h after irradiation RNAs were extracted from each irradiated and non-irradiated well with NucleoSpin™ RNA extraction kit (740955, Macherey-Nagel). Deviating from the protocol, instead of β-mercaptoethanol, 5,25 µl DTT (1 M) was used.

In order to study the effects of *CASP8* mutations on the cytokine expression after being induced by TRAIL, HeLa CASP8-MT/WT cells were plated at the amount of 6 x 10^4 cells /well on 6-well plates, two replicates from each MT cell line and four replicates from WT cell line. Cells were treated with Doxycycline Hyclate (324385-1GM, Merck) 30 ng/ml for 24 h followed by treatment with TRAIL (375-TL, R&D Systems) 50 ng/ml. For each cell line the other replicate was left untreated with TRAIL. After 24 h, RNAs were extracted as above.

2.5.2 cDNA synthesis

cDNA synthesis was performed for the extracted RNAs with SensiFAST cDNA Synthesis Kit (BIO-65054, Meridian Bioscience) according to kit's protocol. 500 ng of RNA was used in the reaction and after cDNA synthesis, reactions were diluted 1:5 in AccuGENE H_2O.

2.5.3 QPCR

Cytokine expressions were detected by QuantStudio™ 3 Real-Time PCR system (Thermo Fisher Scientific) with TaqMan™ Universal Master Mix II, no UNG (4440040, Thermo Fisher Scientific) and TaqMan primers IL-6 (Hs00174131_m1, TFS), IL-8 (Hs00174103_m1, TFS), CXCL1 (Hs00236937_m1, Thermo Fisher Scientific) and GAPDH (Hs02758991_g1, TFS). Also, Caspase-8 mRNA expressions were detected with TaqMan primer (Hs01018151_m1, Thermo Fisher Scientific). 2 µl of cDNA and 1 x TaqMan primers were used in total volume of 10 µl of qPCR reaction. QPCR cycling conditions were as following; +50°C for 2 min, +95°C for 10 min and 40 cycles of +95°C for 15 s, +60°C for 1 min. CT values were normalized to CT values from GAPDH and fold changes were calculated with 2^deltadeltaCt method (Livak & Schmittgen 2001). Results were analysed with Prism GraphPad and Ordinary one-way ANOVA was used to calculate statistical differences. This experiment was repeated three times with irradiation-induced expression and once with TRAIL-induced expression.

2.5.4 Western blotting

Simultaneously as cells were plated for the first and third replicate of irradiation experiment, cells were also plated for western blot. Cell amount and doxycycline treatment (24 h) were as described above (Chapter 2.5.1), and cells were lysed with 70 µl of lysis buffer. Protein concentrations, sample preparation, western blot electrophoresis and imaging were performed as described in Chapter 2.2.1, only difference being that primary antibody Caspase-8 (ab32397, Abcam) was used.

3 Results

3.1 HeLa$^{CASP8-/-}$ clones and characterization

Endogenous *CASP8* was knocked out from HeLa cells with CRISPR/Cas9 -technique. After single-cell cloning and screening with immunoblotting, the absence of CASP8 was detected in six clones, as seen in Figure 6A where numbers indicate different single-cell clones. CASP8 expression in WT HeLa cells was blotted for comparison and it resulted in an expected band in size of 55 kDa. Different HeLa$^{CASP8-/-}$ clones had different morphologies (Fig. 6B). Knock-out (KO) clones #7 and #21 seemed to have similar morphologies, resembling WT HeLa cells. KO clones #18 and #41 were similar to each other, yet differing from WT HeLa cells by growing more sparsely. KO clones #35 and #38 had almost identical morphologies but appeared to grow more in clusters compared to WT HeLa cells.

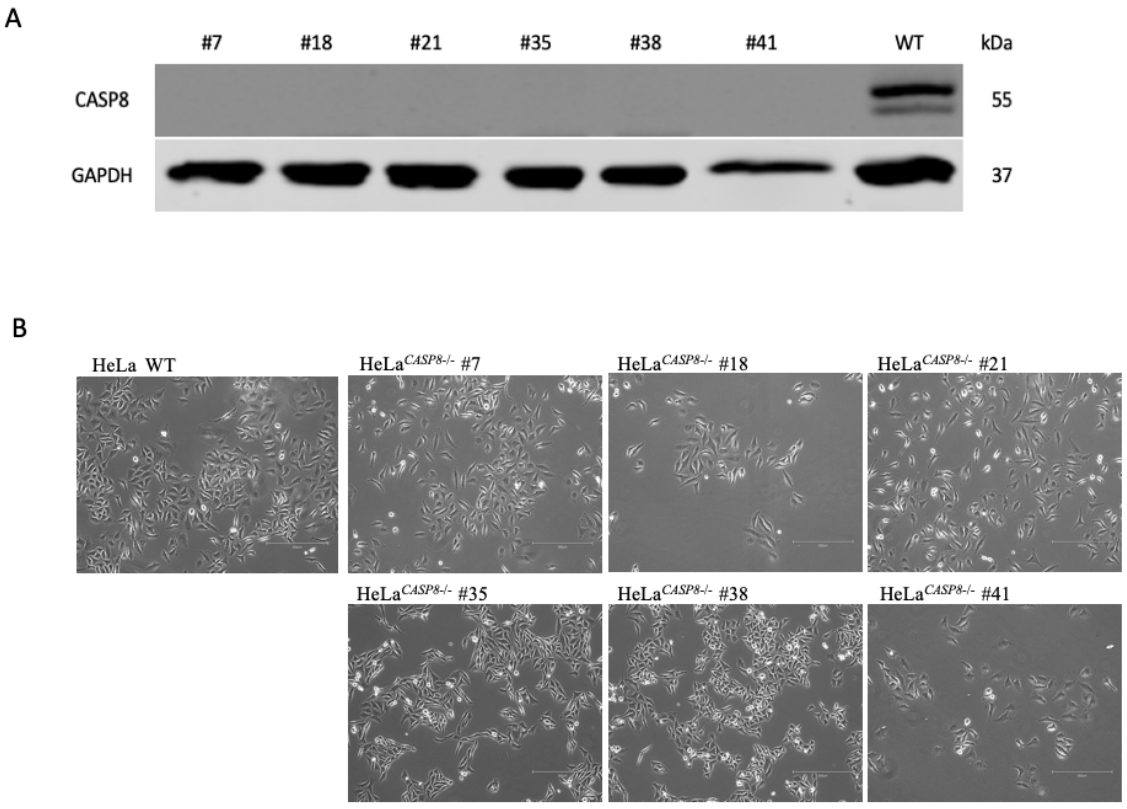

Figure 6. CASP8 expression and morphology of HeLa$^{CASP8-/-}$ clones after knocking out the endogenous *CASP8* with CRISPR/CAS9. Numbers indicate different clones from single-cell cloning. A) Absence of CASP8 expression in HeLa$^{CASP8-/-}$ clones was analyzed by immunoblotting. WT HeLa cells expressed CASP8 (55 kDa) as expected and GAPDH was blotted as a housekeeping protein. B) Morphological differences within HeLa$^{CASP8-/-}$ clones and HeLa WT cells imaged with EVOS M5000 microscope (Thermo Fisher Scientific). KO clones #7 and # 21 resembled HeLa WT cells, whereas #18, #35, #38 and

#41 differed from WT cells by growing more sparsely or in clusters. Dimension line is 300 μm.

In order to select the most suitable HeLa$^{CASP8-/-}$ clone to insert *CASP8* mutations, the six KO clones were characterized by irradiation sensitivity and proliferation. Cells were irradiated with doses of 0, 2, 4, 6 and 8 GY, and cell viabilities were measured after seven days using the MTT assay. The absence of *CASP8* did not seem to have significant effect on the cell viability after irradiation, when compared to WT HeLa cells (Fig. 7A). All HeLa$^{CASP8-/-}$ clones and WT HeLa cells had similar pattern in the cell viability after irradiation; the more radiation cells were exposed to, the more died. Some clones (#7 and #18) had weaker viabilities than WT HeLa with smaller radiation doses, but all cell lines ended up with viability between 20 to 30 % after irradiation dose of 8 GY.

Cell proliferation was characterized by measuring the proliferation on days 1, 3, 5 and 7 (MTT), and normalizing results to proliferation from day 1. Differences in the cell proliferation were noticeable (Fig. 7B). HeLa$^{CASP8-/-}$ clones seemed to form three different patterns in context of proliferation. KO clones #41 and #7 acted the same way whereas #18 and #21 had similarities in proliferation, however all proliferated slower than WT HeLa cells. Only KO clones #35 and #38 appeared to resemble the proliferation of WT HeLa cells.

Based on the properties of irradiation sensitivity and proliferation, as well as morphologies, two KO clones (#21 and #38) were chosen for further characterization. These clones were transiently transfected with plasmids containing WT *CASP8* or GFP in order to detect whether re-expression of exogenous CASP8 was successful. GFP signal was used to evaluate the transfection efficiency. Expression of CASP8 was detected in both cell lines after transfection with *CASP8,* but in GFP-transfected KO clone #38, a band of the same size as WT CASP8's smaller band was detected (Fig. 7C). GFP-transfected KO clone #21 on the other hand did not express CASP8, as expected. Proliferation measurements after *CASP8*-transfection confirmed that re-expression of CASP8 had an effect on KO clone #21 (Fig. 7D). Cells proliferated better than the KO clone #21 cells that did not express CASP8. However, proliferation of these *CASP8*-transfected cells did not reach the proliferation of WT HeLa cells. Moreover, re-expression of CASP8 in KO clone #38 had almost no effect on the cell proliferation.

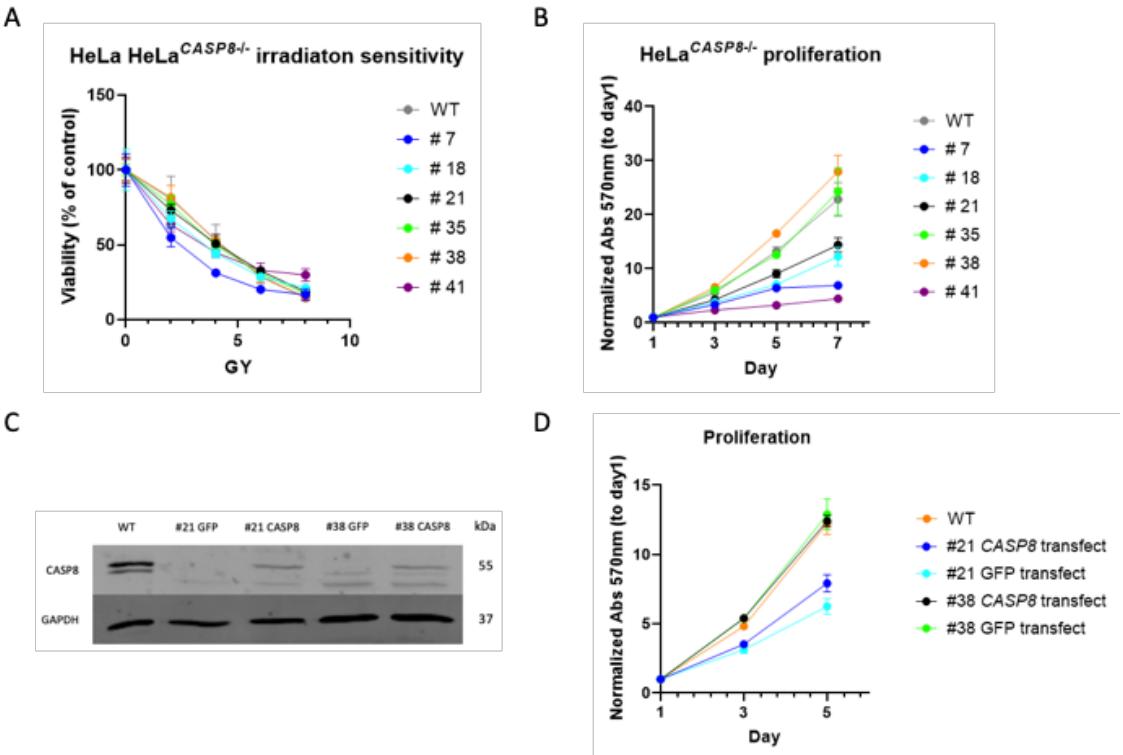

Figure 7. Characterization of the HeLa$^{CASP8-/-}$ cells. Numbers represent the different single-cell clones after knocking out endogenous *CASP8*. A) Irradiation sensitivity measured 7 days after irradiation with doses 0, 2, 4, 6 and 8 GY. Results normalized to 0 GY and error bars represent the SD. B) Proliferation of HeLa$^{CASP8-/-}$ cells measured on days 1, 3, 5 and 7, results normalized to absorbances of day 1 and error bars represent the SD. C) HeLa$^{CASP8-/-}$ cells were transiently transfected with pBABE-*CASP8*/GFP. Immunoblotting revealed faint bands in size of 55 kDa in both knockout cell clones after *CASP8*-transfection, but also in GFP-transfected KO clone #38. WT Hela cells were immunoblotted for comparison. D) Proliferation of *CASP8*- and GFP-transfected cells were measured on days 1, 3 and 5, and normalized to day 1 absorbances (SD error bars). Re-expression of CASP8 had a positive effect on the proliferation of KO clone #21, but almost no effect in the KO clone #38.

Taken together, the aim was to characterize a suitable HeLa$^{CASP8-/-}$ clone to insert *CASP8* mutations. Ideally, the perfect knock-out clone would act and proliferate similarly as WT HeLa cells. Based on proliferation, effect of transient transfection of WT CASP8 and morphology, the KO cell clone #21 was selected for subsequent experiments.

3.2 *CASP8* mutations and stable HeLa CASP8-MT/WT cell lines

CASP8 mutations (L7V, L62P, R71T, S99F, L105H, D303G, S375*, T441I, Q465*) were created with site-directed mutagenesis to pDONR-*CASP8*-Flag plasmid. PCR-products were digested, purified, ligated and finally propagated in competent *E. coli* Dh5α.

Plasmid DNAs were resolved on agarose gel after restriction digestion in order to pre-screen for correct plasmid sizes prior subjecting to Sanger sequencing. Figure 8 illustrates sequence electrophoretograms of nine successful *CASP8* mutation plasmids; L7V, L62P, R71T, S99F, L105H, D303G, S375*, T441I, Q465*. Red box indicates the mutation site and the inserted amino acid mutation. Mutations S375* and Q465* were early stop-codons. Five out of nine mutations (L7V, L62P, R71T, S99F and L105H) were in the prodomain of procaspase-8 and the rest four (D303G, S375*, T441I and Q465*) were in the catalytic domain.

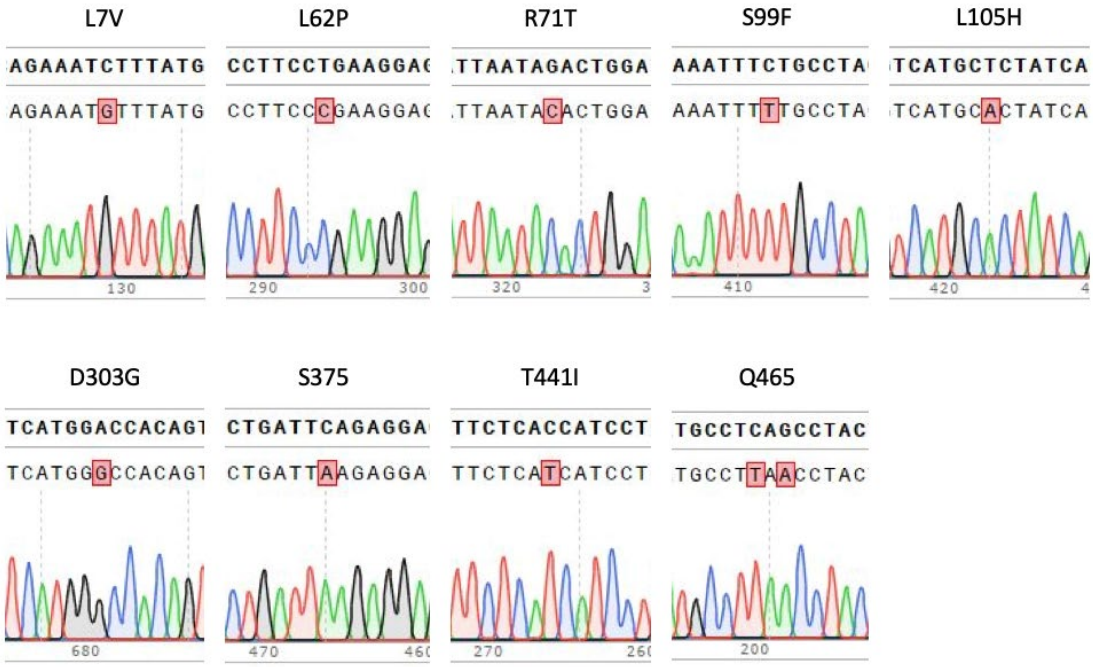

Figure 8. Sequence electrophoretograms of nine different *CASP8* mutations (L7V, L62P, R71T, S99F, L105H, D303G, S375*, T441I, Q465*). Red box indicates the mutation site and the occurred DNA mutation, and the resulting amino acid mutation is shown above. Mutations S375* and Q465* were early stop-codons. Sequence electrophoretograms were analyzed with SnapGene.

CASP8 mutations and WT *CASP8* were cloned from pDONR221-plasmids to destination vector pCW57.1 with Gateway LR cloning. HeLa$^{CASP8-/-}$ cells (clone #21) were virally transduced with the pCW57.1-*CASP8* mutant or wild-type constructs (L7V, L62P, R71T, S99F, L105H, D303G, S375*, T441I, Q465*, WT). Cell morphologies were imaged after successful transduction, as illustrated in Figure 9. Mutation cell line S99F seemed to grow more in clusters, whereas the other mutation cell lines were morphologically quite similar.

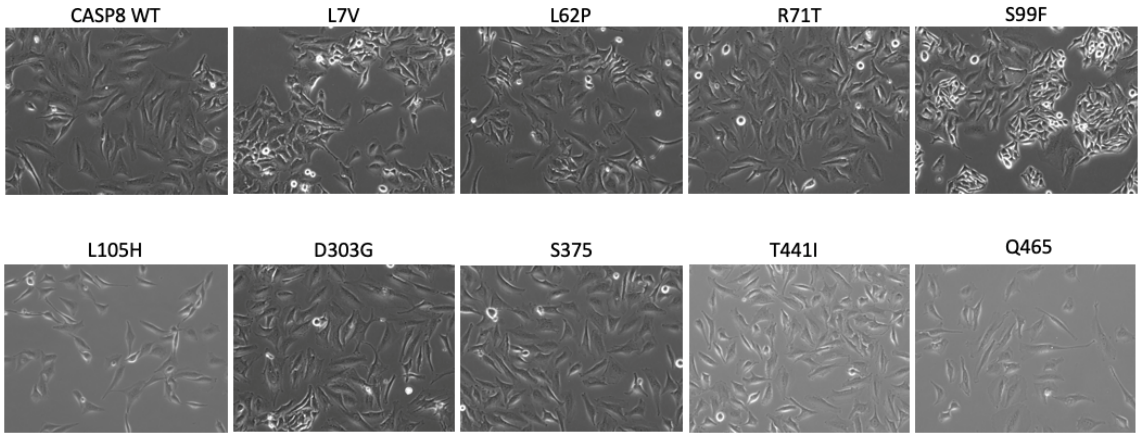

Figure 9. Morphological features of HeLa CASP8-MT/WT cells. Imaged with EVOS M5000 Microscopy (Thermo Fisher Scientific), with 20 x objective. HeLa CASP8-S99F cells grew more as clusters, whereas other *CASP8* mutation cell lines grew similarly as WT HeLa cells.

3.3 Characterization of HeLa CASP8-MT/WT cells

Created HeLa CASP8-MT/WT cell lines expressed mutated CASP8 or WT CASP8 in doxycycline-inducible way. They were characterized by cell viability assays after increased concentrations of doxycycline to ensure that doxycycline-induced expression of CASP8 functions properly, and the insertion of *CASP8* mutations were successful. Increased concentrations of doxycycline revealed that HeLa CASP8-WT cells were more sensitive to this antibiotic and had lower cell viabilities with lower concentrations than HeLa CASP8-MT cell lines (Fig. 10A). Six out of nine *CASP8* mutation cell lines (L7V, L62P, R71T, S99F, L105H and Q465*) did not exhibit lower cell viability after treated with doxycycline (1000 ng/ml) and they tolerated higher levels of doxycycline than HeLa CASP8-WT cells. (Fig. 10B). These mutation cell lines had cell viabilities of 88–105 % after doxycycline treatment when compared to nontreated cells (0 ng/ml dox), whereas the viability of HeLa CASP8-WT cells was 24 %. Mutation cell lines D303G, S375* and T441I exhibited lower cell viabilities and were slightly more sensitive to doxycycline than the six other mutation cell lines, having viabilities between 57 % to 73 % after 1000 ng/ml doxycycline treatment, however still tolerated higher levels of doxycycline than HeLa CASP8-WT cells.

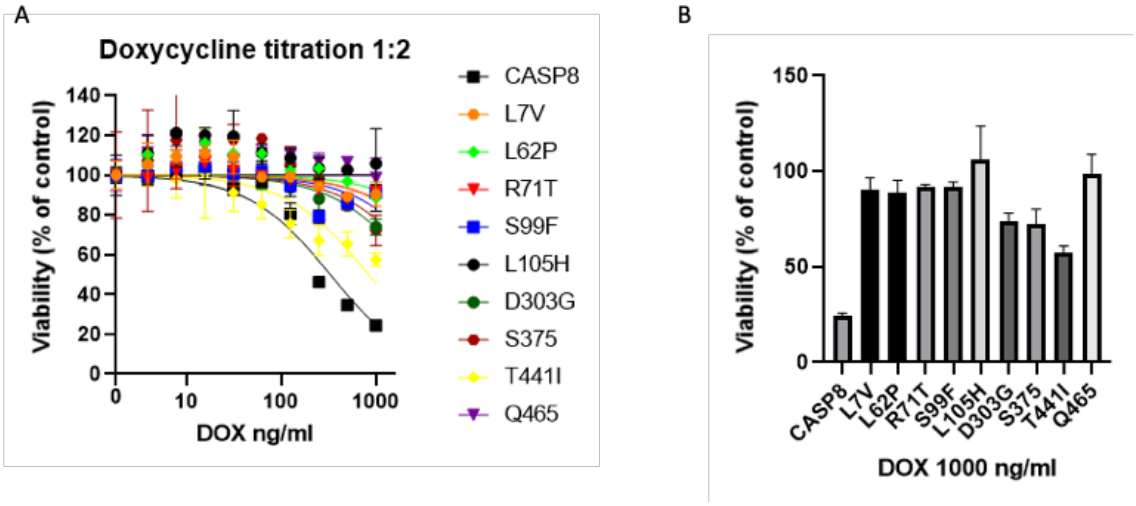

Figure 10. Characterization of doxycycline-inducible HeLa CASP8-MT/WT cell lines by cell viability. A) Increased concentrations of doxycycline (0–1000 ng/ml) for HeLa CASP8-MT/WT cells. Cell viability was measured after 72 h and normalized to absorbances of doxycycline 0 ng/ml. HeLa CASP8-MT cells were more resistant to doxycycline than HeLa CASP8-WT cells. Error bars represent the SD. B) Effect of doxycycline 1000 ng/ml on HeLa CASP8-MT/WT cells. *CASP8* mutation cell lines were more sensitive to doxycycline than cells expressing WT *CASP8*, as expected. Error bars represent the SD.

CASP8 overexpression levels in HeLa CASP8-WT cells were analyzed by western blotting after being treated with doxycycline in concentrations of 0–1000 ng/ml (Fig. 11A). Western blot illustrated the increased expression of CASP8 as doxycycline concentration was increased. Immunoblotting of PARP demonstrated that the more CASP8 was expressed in the cells, the more cleavage of PARP occurred, which was seen as 89 kDa size band. According to the immunoblotting, expression level of endogenous CASP8 (WT HeLa) was reached in HeLa CASP8-WT cells with 30 ng/ml of doxycycline.

Doxycycline-induced CASP8 expressions were analyzed in all mutation cell lines and CASP8-WT cell line by western blotting (Fig. 11B). Cells did not express CASP8 at all when doxycycline was absent, whereas CASP8 expression was reached with doxycycline treatment. Doxycycline concentration of 264 ng/ml was used, and it was based on IC-50 values from previous assays. Mutation cell lines S375* and Q465* expressed truncated CASP8, 40 kDa and 52 kDa respectively, because these mutants harbored premature stop-codons.

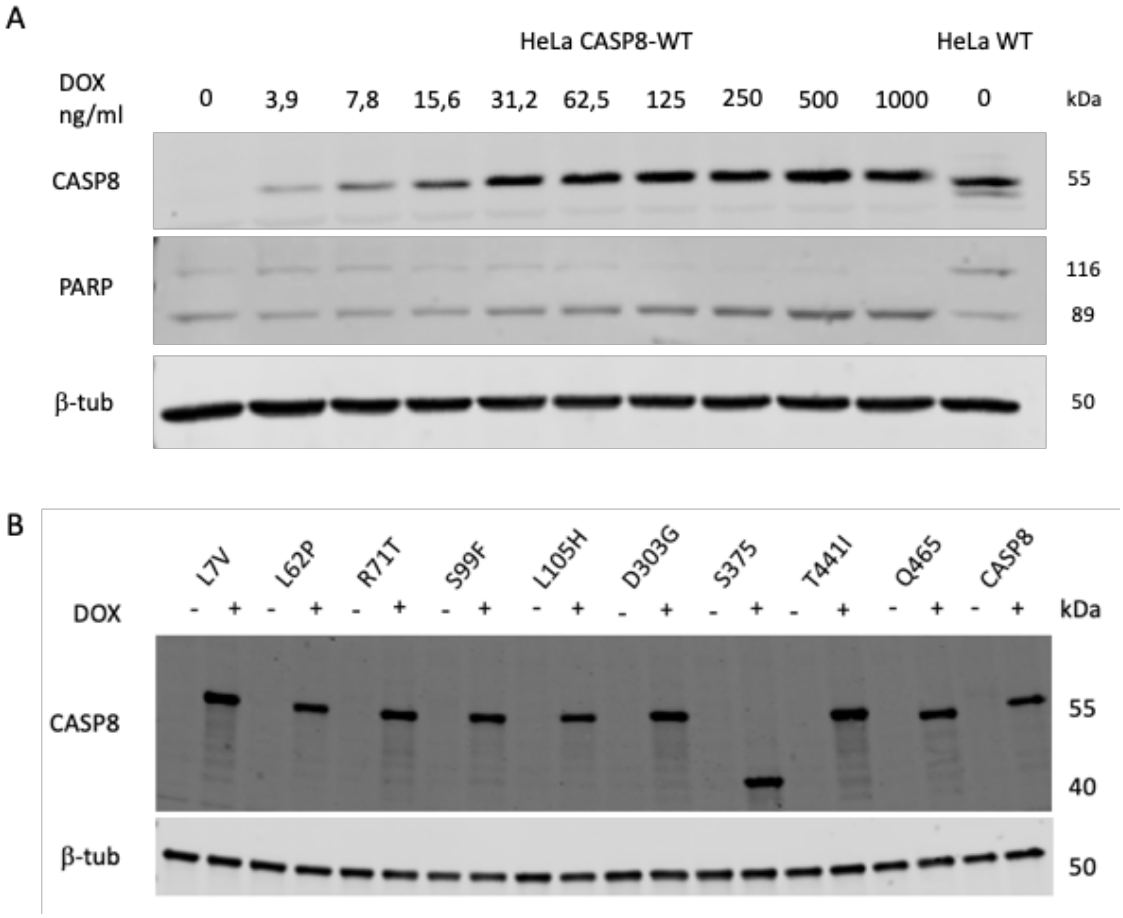

Figure 11. Doxycycline-induced CASP8 expressions in HeLa CASP8-WT cells (marked as CASP8 in figure) and HeLa CASP8-MT cells. *β-tubulin* was blotted as a loading control. A) CASP8 expression in HeLa CASP8-WT cells following increased concentrations of doxycycline. Cells lysed after 24 h of doxycycline treatment. The more doxycycline was present, the more CASP8 was expressed. Overexpression of CASP8 resulted as increased cleavage of PARP, which was seen as cleaved band of 89 kDa instead of full size 116 kDa. B) Expressions of CASP8 with 0 and 264 ng/ml of doxycycline in all HeLa CASP8-MT/WT cell lines. No expression of CASP8 was detected without doxycycline (marked as "-") and clear expressions were observed with doxycycline (marked as "+") with all cell lines.

High levels CASP8-WT can trigger apoptosis in HeLa cells, and high concentrations of doxycycline may be toxic (Fig. 10). For this reason, the concentration of doxycycline to be used in following experiments was carefully analyzed. 30 ng/ml doxycycline in HeLa CASP8-MT/WT cells yielded CASP8 expression levels similar to endogenous CASP8 expression in WT HeLa cells. In addition, the 30 ng/ml of doxycycline had no effect on viability of HeLa CASP8-WT cells. Therefore, 30 ng/ml doxycycline was used in subsequent experiments. All in all, these results confirmed that HeLa CASP8-MT/WT cell lines were viable and the expression of CASP8 was indeed doxycycline-inducible.

These results suggested that created *CASP8* mutation cell lines can be used in subsequent experiments.

3.4 Irradiation-induced cell death in HeLa CASP8-MT/WT

CASP8 mutation cell lines were irradiated with doses 0, 2, 4, 6 and 8 GY, after which cell viabilities were measured using the MTT assay. Some differences in cell viabilities were detected between the cell lines after irradiation, however the differences were relatively modest, as illustrated in Figure 12A. Mutation cell lines T441I and Q465* resisted cell growth inhibition after irradiation to greatest extent, although viabilities were 22.8 % and 22.5 % after 8 GY irradiation, respectively. Mutation cell line L62P had viability of 18.5 % after 8 GY irradiation, while the rest eight cell lines ended up with viabilities of 11–15 %. Surprisingly, no difference in the cell viabilities were detected between CASP8 KO cells and CASP8-WT (marked as CASP8 DOX 0 and CASP8 in Fig. 12A, respectively) after irradiation. Both cell lines had viabilities of 15 % following 8 GY irradiation.

After 4 GY irradiation, five out of nine *CASP8* mutation cell lines (L7V, L62P, R71T, S99F, D303G) exhibited lower cell viabilities than CASP8-WT cells (Fig. 12B). Two mutation cell lines, T441I and Q465*, exhibited greater resistance to irradiation-induced cell death than wild-type cells with statistical significances observed ($P < 0.001$ and $P < 0.05$, respectively). Again, no statistical difference in cell viabilities were detected between CASP8 KO and CASP8 WT cell lines after 4 GY irradiation.

Differences in irradiation sensitivities after 4 GY irradiation could be observed within all cell lines and experiment replicates (Fig. 12C). Mutation cell line Q465* was consistent within all replicates being more resistant to irradiation in relation to CASP8-WT cells. Similarly, T441I exhibited resistance to irradiation to greater extent than CASP8-WT cells, however statistical significance was detected only in one replicate ($p < 0.001$). In relation to CASP8-WT, L105H mutation cell line exhibited irradiation resistance in two experiment replicates, whereas S99F resulted with higher irradiation sensitivity after 4 GY within all replicates. However, statistical differences were not detected in every replicate. Within experiment replicates, mutation cell lines L7V and L62P showed both resistance and sensitivity to irradiation. The irradiation sensitivity of mutations D303G and S375* resembled the sensitivity of CASP8-WT, although in the third experiment replicate both mutations exhibited higher sensitivity to irradiation than wild-type.

Moreover, six out of nine mutation cell lines were more sensitive to irradiation in the third experiment replicate (sensitivity measured six days after irradiation), including D303G and S375*, when compared to CASP8-WT cell line, while in the first and second replicates (sensitivity measured five days after irradiation) only one and three mutation cell lines exhibited irradiation sensitivity greater than CASP8-WT, respectively.

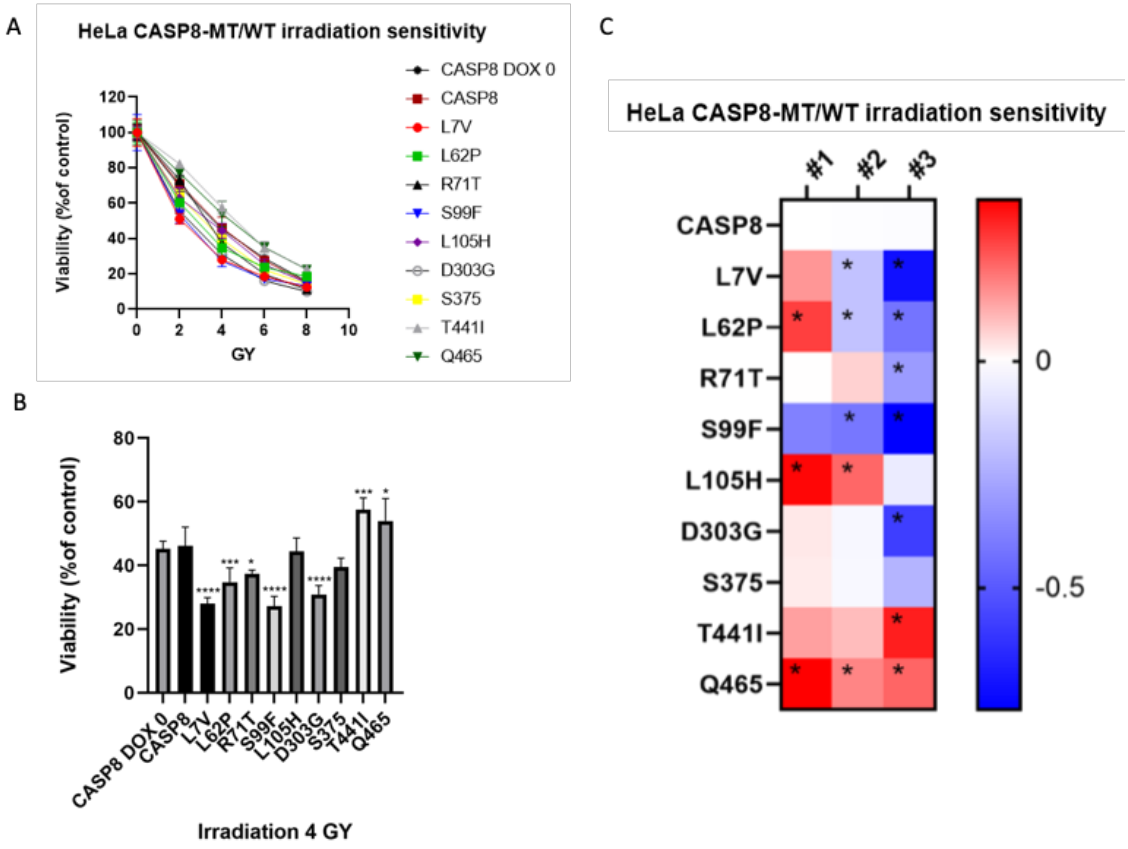

Figure 12. Cell viability in Hela CASP8-MT/WT cells after irradiation with doses of 0, 2, 4, 6 and 8 GY. Cells were treated with 30 ng/ml doxycycline 24 h prior irradiation and throughout the experiment. A) Cell viability measured six days after irradiation (related to 0 GY). Figure is representative for all three individual experiments. Each cell line had five biological replicates within experiments and error bars represent the SD. B) Cell viability after 4 GY irradiation. All cell lines normalized to cell viability after 0 GY. Ordinary one-way ANOVA was used to compare all cell lines to doxycycline treated HeLa CASP8-WT (marked as CASP8 in the figure). Statistical differences were detected in seven out of nine mutation cell lines. T441I and Q465* had higher viabilities than CASP8-WT whereas the rest had lower viabilities after irradiation. C) Heatmap of irradiation sensitivities after 4 GY irradiation in all experiment replicates. Ordinary one-way ANOVA was used to compare all mutation cell lines to CASP8-WT. Asterisks denote the statistical difference and the color indicates the extent of the difference. First and second replicates were five-days experiments and the third was a six-day experiment (#1–3).

Taken together, based on these results two mutation cell lines, T441I and Q465*, conferred mild resistance to irradiation consistently after 4 GY irradiation to greater extent than CASP8-WT. Even though differences were relatively modest, statistical significances were observed. Moreover, no difference in cell viabilities were detected between CASP8 KO and WT cell lines after irradiation.

3.5 NF KB activation in HeLa CASP8-MT/WT cells

3.5.1 Irradiation-induced cytokine and chemokine expression

The effects of *CASP8* mutations on the cytokine and chemokine expression following irradiation were analysed by qPCR. Mutation cell lines L105H, D303G, S375*, T441I and Q465* were detected to induce cytokine and chemokine expression after 8 GY to greater extent than without irradiation (Fig 13A). R71T, S99F, CASP8 KO (marked as -dox in the figure) and CASP8-WT cells retained the cytokine and chemokine expression levels almost similar to without irradiation. Similarly, L7V and L62P mutation cell lines did not show significant induction of cytokine and chemokine expression after 8 GY, however the results were not completely consistent within the experiment replicates.

CASP8 expression was analysed by western blotting which was performed simultaneously with the first and third irradiation experiments. As Figure 13B illustrated, surprisingly not all mutation cell lines (L7V, L62P) expressed CASP8 after induced by doxycycline. Cell lines S99F, L105H and S375* expressed CASP8, albeit relatively weakly. Based on the results from the CASP8 immunoblotting, cell lines that did not express CASP8 were excluded from the cytokine and chemokine expression analysis (Fig. 13C). Cytokine and chemokine expression levels (fold change) after 8 GY irradiation indicated that irradiation enhanced the secretion of IL-6, IL-8 and CXCL1 in nearly all analysed cell lines, including CASP8 KO and CASP8-WT cells. However, in the second experiment replicate mutation cell line S375* increased the expression of all inflammatory factors remarkably, and R71T decreased the expressions of IL-8 and CXCL1. Similarly, in the second replicate mutation cell line T441I decreased IL-8 expression remarkably after irradiation. However, these findings could only be detected in one out of three experiment replicates and two other replicates (# 1 and 3) showed increased cytokine and chemokine expression levels after irradiation.

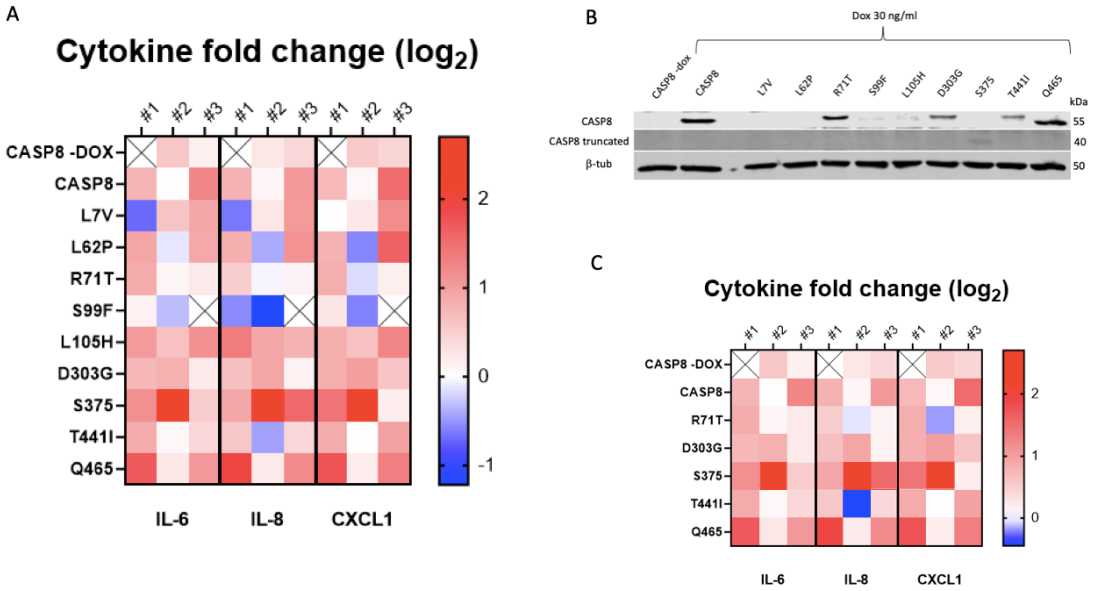

Figure 13. The expression of cytokines IL-6, IL-8 and CXCL1 in HeLa CASP8-MT/WT cells after 8 GY irradiation. Cells were treated with 30 ng/ml doxycycline 24 h prior irradiation and throughout the experiment. A) Log_2 fold change in cytokine expression in HeLa CASP8-MT/WT cells after 8 GY irradiation compared to non-irradiated control cells (0 GY) and normalized to *GAPDH* expression. Triplicates from each cell line in each experiment (#1–3). X-boxes mark unreliable CT values from qPCR due to non-consistent CT values from the reference gene (*GAPDH*). B) Immunoblotting of CASP8 in HeLa CASP8-MT/WT cell lines. Representative western blot for two experiment replicates. C) Cytokine expression in HeLa CASP8-MT/WT cells after 8 GY. Data presented as in (A). Cell lines that expressed CASP8 (according to western blot) are shown in the heatmap.

All in all, these data argue that *CASP8* mutations could enhance the secretion of cytokines and chemokines IL-6, IL-8 and CXCL1 after irradiation. Based on these results mutations in the catalytic domain of Caspase-8 could enhance the induction of these inflammatory factors to slightly greater extent than mutations in the prodomain. However, also CASP8 KO cells (-dox) enhanced the induction of cytokines and chemokines after irradiation, although relatively weakly.

3.5.2 TRAIL-induced cytokine and chemokine expressions

The effect of *CASP8* mutations on the expression of cytokines and chemokines IL-6, IL-8 and CXCL1 after being induced by TRAIL were analyzed by qPCR. Figure 14 illustrated that increased induction of the cytokines and chemokines following TRAIL

treatment was seen in almost all cell lines expressing CASP8 mutants. Especially mutations in the catalytic domain (D303G, S375*, T441I, Q465*) enhanced the secretion up to 1,5-fold in relation to 0 ng/ml TRAIL. Decreased production of IL-6, IL-8 and CXCL1 was seen in mutation cell line L62P after treatment with TRAIL. L7V showed decreased expression of IL-6 while slightly increased the expressions of IL-8 and CXCL1. Prodomain mutation L105H increased the cytokine and chemokine expression after TRAIL treatment. Similarly did the prodomain mutation S99F, although the expression of CXCL1 was slightly decreased. CASP8 KO cells (CASP8 -DOX in the figure) showed decreased expression of IL-6 while expressions of IL-8 and CXCL1 remained nearly unchanged in relation to no TRAIL treatment. Moreover, CASP8-WT cells (CASP8 in the figure) showed enhanced expression of all three cytokines and chemokines after TRAIL treatment. Taken together, seven out of nine *CASP8* mutations enhanced the expression of IL-6, IL-8 and CXCL1 after TRAIL treatment and mutation L62P decreased the expression of these inflammatory factors.

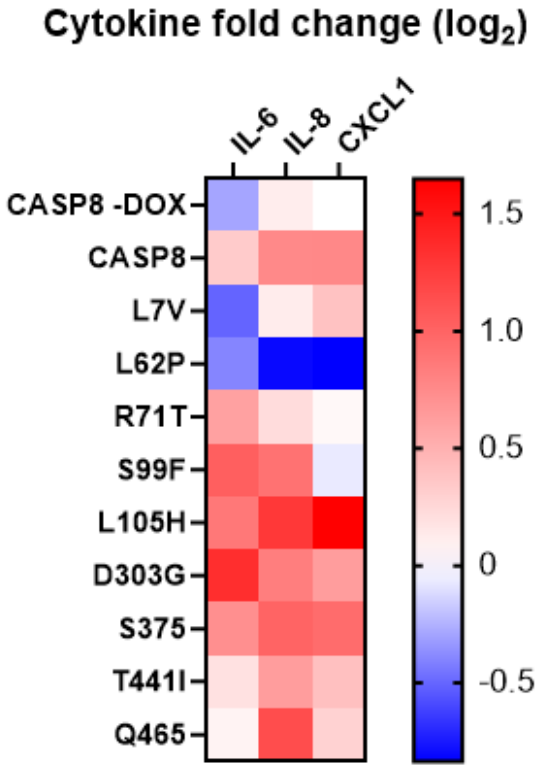

Figure 14. Cytokine expression (log_2 fold change to untreated control cells) in HeLa CASP8-MT/WT cell lines induced by TRAIL (50 ng/ml, 24 h). Cytokines IL-6, IL-8 and CXCL1 were detected from mRNA after -/+ TRAIL treatment. Cells were treated with doxycycline (30 ng/ml) 24 h prior to TRAIL treatment. HeLa CASP8-WT were also treated with TRAIL without CASP8 induction (marked as CASP8 -DOX).

4 Discussion

This thesis aimed to investigate nine HNSCC-associated *CASP8* mutations and their effect on radiotherapy and inflammation response following death receptor stimulation in cancer cells. Previously, *CASP8* mutations have been shown to impair the apoptotic signaling after death receptor activation (Li et al. 2014; Cui et al. 2021). Mutations in this gene have also been shown to induce the activation of NF-κB signaling pathway to greater extent than WT CASP8, and thus promote expression of inflammatory cytokines and chemokines (Ando et al. 2013; Cui et al. 2021). According to TCGA database, presence of *CASP8* mutations in tumors are associated with poor survival (Fig. 1). In this study, the contribution of HNSCC-associated *CASP8* mutations (L7V, L62P, R71T, S99F, L105H, D303G, S375*, T441I and Q465*) to radiotherapy response was investigated. Aim was to determine whether some of the nine HNSCC-associated *CASP8* mutations confer resistance to irradiation. In addition, the effect of the *CASP8* mutations on inflammatory signaling mediated by death receptor stimulation in cancer cells was studied.

4.1 Irradiation-mediated apoptosis in HeLa CASP8-MT/WT cells

CASP8 mutations are associated with poor overall survival and prognosis of HNSCC patients, especially when patients are solely treated with radiotherapy, as illustrated in Figure 1. Previous studies suggest that *CASP8* mutations could inhibit the activation of apoptotic signaling and cell death following activation of death receptors (Li et al. 2014; Cui et al. 2021). In addition, HNSCC cell lines harboring *CASP8* mutations have been shown to be more resistant to irradiation than those with wild-type *CASP8* (Uzunparmak et al. 2020). It is of great importance to study and identify the limiting factors in cell death sensitivity and radiotherapy resistance.

Two out of nine *CASP8* mutations (T441I and Q465*) resisted cell growth inhibition following irradiation to greater extent than WT CASP8, suggesting that these mutations could potentially impair the activation of apoptotic signaling pathway after irradiation (Fig. 12). This further indicates that cells expressing *CASP8* mutants could most likely confer resistance to irradiation-mediated cell death. Noteworthy is that also mutation L62P exhibited higher cell viability than WT CASP8, although only with 8 GY irradiation. Seven out of nine *CASP8* mutations were more sensitive to irradiation than

WT CASP8, and of which five with statistical significance (L7V, L62, R71T, S99F and D303G). This finding indicates that these mutations could enhance the apoptotic signaling following irradiation, therefore reduce the cell viability of cancer cells and even enhance the effects of radiotherapy.

Irradiation induces irreparable DNA damage in cells which activates tumor suppressor *P53*, further leading to transactivation of death receptor and assembly of DISC complex (Roos & Kaina 2013). As mentioned earlier, procaspase-8 is required for formation of DISC, and both dimerization and cleavage of the zymogen are required for activation of apoptotic signaling. Since both irradiation and TRAIL-ligand may stimulate death receptor activation and therefore potentially activation of extrinsic apoptotic signaling, studies based on TRAIL-induced death receptor activation could be applied to the interpretation of cell death potentially induced by irradiation. However, noteworthy is that resistance to TRAIL-induced cell death does not necessarily mean resistance to irradiation mediated cell death.

Previously, mutations T441I and Q465* have shown to resist cell growth inhibition following TRAIL treatment (Cui et al. 2021). Similarly, this thesis study resulted that these mutations exhibited higher cell viability than WT CASP8 after irradiation. The mechanism by which these mutations could potentially cause inhibition of cell death signaling still remains obscure. Cui et al. demonstrated that, regarding the catalytic domain mutations, inhibition of death signaling is not most likely due to defective dimerization since the mutations they studied retained the ability to dimerize with WT procaspase-8. In contrary, Li et al. (2014) showed reduced capacity of *CASP8* mutation S375* to form dimers with WT procaspase-8, which could enable this mutation to resist cellular death following death receptor activation. Here, S375* resembled WT CASP8 in the context of cell viability after irradiation and irradiation sensitivity, with only modest differences observed (Fig. 12). This finding however, was inconsistent with the previous studies (Li et al. 2014; Cui et al. 2021). Moreover, here missense mutation L105H exhibited higher cell viability after irradiation in relation to WT CASP8, which was consistent with results from Li at al. as well as Cui et al. However, this finding was noticeable only with two first irradiation experiment replicates where cell viability and irradiation sensitivity were measured five days after irradiation. The possible inhibitory mechanism of mutations L62P and L105H remains unclear but most likely could be due to defective dimerization capacity (Cui et al. 2021) or defective cleavage of the zymogen.

Consistently with previous findings form Cui et al., mutations L7V and S99F showed reduced cell viability after irradiation to greater extent than WT CASP8, and these mutations were more sensitive to irradiation. Conversely, in this study mutations L62P, R71T and D303G did not exhibit similar manners in possible cell death activation following irradiation as in previous studies. These three mutations were previously shown to exhibit resistance to TRAIL-induced apoptosis (Cui et al. 2021). However, here L62P, R71T and D303G exhibited lower cell viability in relation to WT CASP8 following 4 GY irradiation (Fig. 12B). Moreover, R71T and D303G retained similar irradiation sensitivities after 4 GY than WT CASP8, although only with experiments where sensitivities were measured five days after irradiation (Fig. 12C). The irradiation sensitivity of mutation L62P varied regardless of the length of the experiment.

Here, the effect of studied nine *CASP8* mutations on the potential activation of apoptotic signaling following irradiation have been interpreted according to previous results from TRAIL-induced cell death signaling. However, it cannot be assumed that irradiation and TRAIL would elicit a completely similar response in cells, so the inconsistency in results may be due to this. Moreover, including a positive control cell line, which is known to resist irradiation in irradiation experiments, would give more answers about the extent of the differences in cell viabilities. Comparing results from this study with positive control would demonstrate whether irradiation and potentially cell death resistance observed in mutations T441I and Q465* could be biologically relevant, in addition to being statistically significant.

4.2 Activation of NF-κB signaling in HeLa CASP8-MT/WT cells

The NF-κB signaling is a key pathway in inflammatory signaling, cell proliferation and differentiation. Caspase-8 plays a crucial scaffolding role in inflammatory signaling independently from its catalytic activity (Henry & Martin 2017). As mentioned earlier, Caspase-8 is required to the formation of FADDosome and subsequent inflammatory signaling. Previous studies have shown that in addition to apoptosis, TRAIL is capable to induce NF-κB-dependent inflammatory signaling and secretion of cytokines and chemokines in HeLa cells (Henry & Martin 2017). Again, since both irradiation and TRAIL-ligand may stimulate the death receptor activation and further formation of FADDosome, studies based on TRAIL-induced inflammatory signaling activation could

be applied to interpretation of potential irradiation-induced activation of the NF-κB signaling pathway. However, conclusions based on these interpretations need to be done with caution since it is not certain that these two mechanisms induce the cytosolic downstream signaling in a completely similar manner.

Mutations L7V, L62P, S99F and L105H were excluded from the final interpretation of irradiation-induced cytokine and chemokine expressions (Fig. 13C) since CASP8 expression was not observed or was relatively modest, based on immunoblotting (Fig. 13B). Reason why the doxycycline-induced expression faded remains unclear. Overall, all analyzed *CASP8* mutations (R71T, D303G, S375, T441I and Q465*) retained the ability to induce cytokines and chemokines (IL-6, IL-8 and CXCL1) following irradiation. Although, R71T reduced the expression of IL-8 and CXCL1 after irradiation, as well as mutation T441I decreased the expression of IL-8 following irradiation, these findings could only be observed in one experiment replicate out of three. Following TRAIL-mediated activation of the death receptor, all catalytic domain mutations retained the ability to induce expression of IL-6, IL-8 and CXCL1 (Fig. 14). Similarly, did almost all prodomain mutations, except L7V with IL-6, and L62P with all three inflammatory factors.

Previous findings by Cui et al. demonstrated that mutations R71T, T441I and Q465* failed to mediate NF-κB signaling after TRAIL treatment while mutations D303G and S375* mediated the induction of cytokines and chemokines even greater than two-fold. Here, results are not completely consistent with these aforementioned findings by Cui et al. since retained ability to induce NF-κB signaling was observed with R71T, T441I and Q465*. Moreover, TRAIL-mediated cytokine and chemokine expression revealed that these three mutations were capable to induce the secretion of IL-6, IL-8 and CXCL1 to slightly greater extent than without death receptor activation (Fig. 14). In previous studies by Cui et al., L62P upregulated expression of all three inflammatory factors whereas here, L62P decreased the induction of cytokines and chemokines mediated by TRAIL. These inconsistencies might be due to the different mechanism in possible death receptor activation or to inconsistency within experiment replicates, which is possibly due to differences in mRNA purity and quality.

As in previous studies by Cui et al., also here induction of IL-6, IL-8 and CXCL1 after irradiation and TRAIL was seen in cells expressing WT CASP8 (Fig. 13 and 14). However, similar induction was seen in CASP8 KO cells (-dox), although to only modest

extent, which is contrary to the previous studies. This could indicate that the effect of *CASP8* mutations on the irradiation-mediated cytokine and chemokine secretion might not be that relevant in HNSCC. In order to obtain completely reliable conclusions, further experiment to study this topic would be necessary.

The hypothesis of the second aim was that mutations in the catalytic domain could enhance the activation of NF-κB signaling, and thereby induce the expression of inflammatory cytokines and chemokines, whereas mutations in the prodomain could impair the inflammatory signaling. This was based on the previous findings by Ando et al. (2013) and Cui et al. (2021), as well as the observation by Henry & Martin (2017) suggesting that oligomerization of proaspase-8 molecules in formation of FADDosome occur via DED2-DED2 interaction. Thus, it could be suggested that mutations in the prodomain could impact the formation of FADDosome and therefore impair downstream NF-κB signaling. Missense mutation L105H is located in the DED2 domain of procaspase-8 and therefore a single amino acid change seems to be enough to affect negatively the death receptor-mediated inflammatory signaling (Cui et al. 2021). In this study however, mutation L105H retained the ability to induce IL-6, IL-8 and CXCL1 following irradiation (Fig. 13A) and TRAIL (Fig. 14), although the expression of mutant CASP8 was relatively weak. Moreover, previous study by Li et al. (2014) demonstrated that mutation L105H conferred resistance to apoptosis in vitro, while promoted cell growth and metastasis in vivo, indicating complex impact of *CASP8* mutations in cancer cells.

CASP8 mutations in tumors could shift the downstream signaling of death receptor from apoptotic to inflammatory and therefore promote migration and proliferation of cancer cells (Henry & Martin 2017). Moreover, upregulation of inflammatory cytokines and chemokines could promote the TME into more favorable milieu for cancer cells (Cui et al. 2021), and further promote cancer invasion. Conversely, for instance in ovarian cancer, increased activation of the NF-κB pathway and promoted inflammation signaling can improve the outcome of patients (Kim et al. 2016). As previous studies have shown, *CASP8* mutations are not only loss-of-function but individual mutations have different functional properties (Cui et al. 2021). In this study, mutations T441I and Q465* exhibited higher cell viability following irradiation, while retained the ability to induce cytokines and chemokines after irradiation. These findings support the previously observed different functional characters of *CASP8* mutations.

4.3 HeLa CASP8-MT/WT cell lines

In order to study the exact effects of *CASP8* mutations on irradiation and inflammatory responses in cancer cells, the endogenous *CASP8* was knocked from HeLa cells. Surprisingly, the absence of *CASP8* did not seem to have significant effect on the cell viability following irradiation in relation to WT HeLa cells (Fig. 7A). It was assumed that HeLa$^{CASP8-/-}$ cells would resist cell growth inhibition after possible death receptor stimulation to slightly greater extent than WT HeLa cells since the KO cells lack Caspase-8-dependent apoptotic signaling. However, HeLa$^{CASP8-/-}$ cells exhibited lower cell viability after irradiation similarly as WT HeLa cells. Similar findings were observed also in subsequent experiments. No differences in cell viabilities following irradiation were detected between cells expressing WT CASP8 and cells that lacked CASP8 expression (Fig. 12B). Even though, previous study by Cui et al. (2021) have shown that HeLa$^{CASP8-/-}$ cells resisted cell growth inhibition after death receptor activation mediated by TRAIL, irradiation may induce different destruction mechanisms in the cell.

Moreover, contrary to observations by Cui et al., here HeLa cells expressing WT CASP8 did not react to TRAIL-mediated death receptor activation with cell growth inhibition (data not shown). In other words, no differences were detected in cell viabilities following TRAIL treatment between CASP8 KO cells and cells expressing exogenous WT CASP8. To verify that these aforementioned findings were not restricted to the HeLa$^{CASP8-/-}$ clone (#21) used in this study, other HeLa$^{CASP8-/-}$ clones were subsequently characterized in more detail by other group members of KurppaLab. HeLa$^{CASP8-/-}$ clones (#18, 35 and 38) were transduced with WT *CASP8* and the generated cell lines were characterized by increased concentration of TRAIL (data not shown). The results were similar to those previously obtained, cells expressing exogenous WT CASP8 did not react to TRAIL with clear cell growth inhibition. It was assumed that cells expressing WT CASP8 would react to TRAIL-mediated death receptor activation with cell growth inhibition similarly to WT HeLa cells. However, results from these TRAIL experiments (data not shown) indicated that cells expressing exogenous WT CASP8 reacted to TRAIL-mediated death receptor activation only with modest cell growth inhibition regardless of the HeLa$^{CASP8-/-}$ clone. All in all, these verifications proved that results from this study are most likely not restricted to the HeLa$^{CASP8-/-}$ clone used.

One possible reason why HeLa$^{CASP8-/-}$ cells and HeLa CASP8-WT cells without doxycycline treatment (CASP8 KO) did not react to TRAIL-mediated death receptor

stimulation or irradiation as assumed might be linked to necroptosis. Caspase-8 plays a role as an inhibitor of necroptosis by cleaving RIPK1 and CYLD and can therefore regulate the balance between apoptotic signaling and necroptosis (Berghe et al. 2014; Tummers & Green 2017). Since HeLa$^{CASP8-/-}$ cells and HeLa CASP8-WT cells without doxycycline are lacking CASP8 expression, no inhibition of necroptosis is occurring. This cellular process could explain why no differences were observed in -/+ doxycycline treated HeLa CASP8-WT cells in cell viabilities after irradiation (Fig. 12B). Furthermore, irradiation has been shown to induce necroptosis in other cancer types (Wang et al. 2018), and study by Uzunparmak et al. (2020) revealed that in HNSCC cell line inhibition of *CASP8* led to necroptotic cell death. In order to confirm or rule out this reflection, further studies with heterozygous mutations and overexpression of WT CASP8 would be necessary.

Despite these above-mentioned observations, generated HeLa CASP8-MT/WT cell lines reacted to increased concentrations of doxycycline as expected and consistently with previous findings (Cui et al. 2021). HeLa CASP8-MT cells tolerated higher levels of doxycycline than HeLa CASP8-WT cells (Fig. 10), indicating that these HNSCC-associated *CASP8* mutations could fail to induce cell death to some extent. Same data also showed that the exogenous overexpression of WT CASP8 was functioning as expected and was successful in inducing apoptosis. The exogenous expression of WT CASP8 in HeLa cells showed to mediate apoptotic signaling (Fig. 11A). Cleavage of PARP is a sign of apoptosis as executioner Caspases 3 and 7 cleave PARP-1 (Chaitanya et al. 2010). Even though, the generated stable HeLa CASP8-MT/WT cell lines were viable and expressing CASP8 in a doxycycline-inducible way, the expression was lost in subsequent experiments in two mutation cell lines (Fig. 13B). The reason why this occurred remains unknown, however the role of fitness selection in cell culture cannot be ruled out.

4.4 *CASP8* mutations in HNSCC

CASP8 mutations usually occur in HNSCC patients as heterozygous (Pickering et al. 2013) and are known to behave in a dominant-negative manner (Li et al. 2014; Cui et al. 2021). Here in this study, homozygous *CASP8* mutations were studied, and in order to implement results to HNSCC patient data, further studies about heterozygous mutations are required. Heterozygous knock-in mutation L105H and overexpression of WT CASP8

were later studied in HeLa cells by KurppaLab. Their unpublished data demonstrated that cell viability of heterozygous L105H mutation did not differ remarkably from WT CASP8 following increased concentrations of TRAIL. L105H mutation cell line reacted to TRAIL-induced death receptor stimulation with cell growth inhibition, contrary to the assumptions based on previous findings (Li et al. 2014; Cui et al. 2021). Same unpublished data showed that overexpression of WT CASP8 enhanced the activation of apoptotic signaling to greater extent in relation to the endogenous baseline expression of WT CASP8 after death receptor activation by TRAIL. These results indicate that the exogenous expression of WT CASP8 in generated stable cell lines might differ from expression in WT HeLa cells. This could be noted as a one limitation of this study.

As mentioned earlier, the expression of Caspase-8 is rarely completely lost in cancer cases, however the apoptotic activity is altered through different mechanisms, including mutations and posttranslational modifications (Mandal et al. 2020). In OSCC cases CASP8 expression can be either down- or up-regulated due to truncation, missense and non-start mutations (Mandal et al. 2020), indicating the complex role of different *CASP8* mutations. This thesis study also supports the notion that *CASP8* mutations alter the apoptotic signaling rather than inhibit the protein expression completely.

CASP8 mutations are clearly correlated with poor prognosis of HNSCC patients, however based on these results they might not be the sole cause of radiotherapy resistance. The stage of the disease of HNSCC patient and HPV-status might affect the response of cancer therapies, as well as accumulation of other mutations. Co-mutations in genes involved in the death receptor signaling and apoptosis might also play a pivotal role in developing resistance to cell death mediated cancer therapies. Mutations in TRAIL encoding gene *TNFSF10* and in tumor suppressor gene *TP53* as well as amplifications in *FADD* have been observed in HNSCC (Raudenská et al. 2021), and these all could also affect the apoptotic signaling after death receptor stimulation by irradiation.

In summary, findings form this thesis demonstrate that HNSCC-associated mutations can affect the apoptotic and inflammatory signaling following irradiation. Based on the findings from this research, only mutations T441I and Q465* exhibited higher cell viability following irradiation, while retaining the ability to induce the NF-κB-dependent inflammatory signaling. The precise effects of *CASP8* mutations on cell death signaling, and whether there are differences in pro- and catalytic domain mutations in mediating inflammatory signaling, should be further investigated in cell lines derived from HNSCC

patients. Moreover, further studies are also required in order to investigate whether mutations T441I and Q465* could serve as predictive markers in HNSCC. All in all, cancer is a complex disease and many factors can contribute to the development of therapy resistance. Thus, it is of great importance and demand to identify limiting factors in cell death signaling, and to recognize markers to predict the outcome of cancer patients.

Acknowledgments

First of all, I would like to thank my supervisors Kari Kurppa and Päivi Koskinen for expert guidance and support throughout this thesis project. Especially, the sincerest thanks to Kari Kurppa for giving me the opportunity to work in his lab, for providing instructive feedback and financial support.

I would like to express my greatest gratitude for all KurppaLab members Juuli, Kamal, Mari, Meija, Sarang, Zejia and especially Sini. Thank you for always helping and supporting me in the lab and for providing warm and welcoming atmosphere. Also, I would like to express my gratitude for members of Klaus Elenius group.

Finally, I would like to dedicate warm thanks to my family and friends. I am thankful for your never-ending emotional support and understanding throughout this thesis journey. Special thanks to Janette for her invaluable peer support during long days in the library.

References

Ando, M., Kawazu, M., Ueno, T., Fukumura, K., Yamato, A., Soda, M., Yamashita, Y., Choi, Y. L., Yamasoba, T., & Mano, H. (2013). Cancer-associated missense mutations of caspase-8 activate nuclear factor-κB signaling. *Cancer Science*, *104*(8), 1002–1008. https://doi.org/10.1111/cas.12191

Baud, V., & Karin, M. (2009). Is NF-κB a good target for cancer therapy? Hopes and pitfalls. *Nature Reviews Drug Discovery 2009 8:1*, *8*(1), 33–40. https://doi.org/10.1038/nrd2781

Berghe, T. Vanden, Linkermann, A., Jouan-Lanhouet, S., Walczak, H., & Vandenabeele, P. (2014). Regulated necrosis: the expanding network of non-apoptotic cell death pathways. *Nature Reviews Molecular Cell Biology 2014 15:2*, *15*(2), 135–147. https://doi.org/10.1038/nrm3737

Cadoni, G., Boccia, S., Petrelli, L., Di Giannantonio, P., Arzani, D., Giorgio, A., De Feo, E., Pandolfini, M., Gallì, P., Paludetti, G., & Ricciardi, G. (2012). A review of genetic epidemiology of head and neck cancer related to polymorphisms in metabolic genes, cell cycle control and alcohol metabolism. *Acta Otorhinolaryngologica Italica*, *32*(1), 1–11. https://www.ncbi.nlm.nih.gov/pmc/articles/PMC3324962/

Califano, J., van der Riet, P., Westra, W., Nawroz, H., Clayman, G., Piantadosi, S., Corio, R., Lee, D., Greenberg, B., Koch, W., & Sidransky, D. (1996). Genetic progression model for head and neck cancer: Implications for field cancerization. *Cancer Research*, *56*(11), 2488–2492.

Cerami, E., Gao, J., Dogrusoz, U., Gross, B. E., Sumer, S. O., Aksoy, B. A., Jacobsen, A., Byrne, C. J., Heuer, M. L., Larsson, E., Antipin, Y., Reva, B., Goldberg, A. P., Sander, C., & Schultz, N. (2012). The cBio cancer genomics portal: an open platform for exploring multidimensional cancer genomics data. *Cancer Discovery*, *2*(5), 401–404. https://doi.org/10.1158/2159-8290.CD-12-0095

Chaitanya, G. V., Alexander, J. S., & Babu, P. P. (2010). PARP-1 cleavage fragments: signatures of cell-death proteases in neurodegeneration. *Cell Communication and Signaling, 8*(31). https://doi.org/10.1186/1478-811X-8-31

Chang, D. W., Xing, Z., Pan, Y., Algeciras-Schimnich, A., Barnhart, B. C., Yaish-Ohad, S., Peter, M. E., & Yang, X. (2002). c-FLIPL is a dual function regulator for caspase-8 activation and CD95-mediated apoptosis. *The EMBO Journal*, *21*(14), 3704–3714. https://doi.org/10.1093/EMBOJ/CDF356

Cui, Z., Dabas, H., Leonard, B. C., Shiah, J. V., Grandis, J. R., & Johnson, D. E. (2021). Caspase-8 mutations associated with head and neck cancer differentially retain functional properties related to TRAIL-induced apoptosis and cytokine induction. *Cell Death and Disease*, *12*(8). https://doi.org/10.1038/s41419-021-04066-z

Declercq, W., vanden Berghe, T., & Vandenabeele, P. (2009). RIP Kinases at the Crossroads of Cell Death and Survival. *Cell*, *138*(2), 229–232. https://doi.org/10.1016/j.cell.2009.07.006

Dickens, L. S., Boyd, R. S., Jukes-Jones, R., Hughes, M. A., Robinson, G. L., Fairall, L., Schwabe, J. W. R., Cain, K., & MacFarlane, M. (2012). A Death Effector Domain Chain DISC Model Reveals a Crucial Role for Caspase-8 Chain Assembly in Mediating Apoptotic Cell Death. *Molecular Cell*, *47*(2), 291–305. https://doi.org/10.1016/j.molcel.2012.05.004

Elrod, H. A., Fan, S., Muller, S., Chen, G. Z., Pan, L., Tighiouart, M., Shin, D. M., Khuri, F. R., & Sun, S. Y. (2010). Analysis of Death Receptor 5 and Caspase-8 Expression in Primary and Metastatic Head and Neck Squamous Cell Carcinoma and Their Prognostic Impact. *PLOS ONE*, *5*(8), 12178. https://doi.org/10.1371/JOURNAL.PONE.0012178

Freedman, N. D., Park, Y., Subar, A. F., Hollenbeck, A. R., Leitzmann, M. F., Schatzkin, A., & Abnet, C. C. (2008). Fruit and vegetable intake and head and neck cancer risk in a large United States prospective cohort study. *International Journal of Cancer*, *122*(10), 2330-2336. https://doi.org/10.1002/ijc.23319

Fulda, S. (2009). Caspase-8 in cancer biology and therapy. *Cancer Letters*, *281*(2), 128–133. https://doi.org/10.1016/j.canlet.2008.11.023

Gao, J., Aksoy, B. A., Dogrusoz, U., Dresdner, G., Gross, B., Sumer, S. O., Sun, Y., Jacobsen, A., Sinha, R., Larsson, E., Cerami, E., Sander, C., & Schultz, N. (2013). Integrative analysis of complex cancer genomics and clinical profiles using the cBioPortal. *Science Signaling*, *6*(269). https://doi.org/https://doi.org/10.1126%2Fscisignal.2004088

Guha, N., Boffetta, P., Wünsch Filho, V., Eluf Neto, J., Shangina, O., Zaridze, D., Curado, M. P., Koifman, S., Matos, E., Menezes, A., Szeszenia-Dabrowska, N., Fernandez, L., Mates, D., Daudt, A. W., Lissowska, J., Dikshit, R., & Brennan, P. (2007). Oral health and risk of squamous cell carcinoma of the head and neck and esophagus: Results of two multicentric case-control studies. *American*

Journal of Epidemiology, *166*(10), 1159–1173. https://doi.org/10.1093/aje/kwm193

Guicciardi, M. E., & Gores, G. J. (2009). Life and death by death receptors. *The FASEB Journal*, *23*(6), 1625–1637. https://doi.org/10.1096/FJ.08-111005

Hanahan, D. (2022). Hallmarks of Cancer: New Dimensions. *Cancer Discovery*, *12*(1), 31–46. https://doi.org/10.1158/2159-8290.CD-21-1059

Henry, C. M., & Martin, S. J. (2017). Caspase-8 Acts in a Non-enzymatic Role as a Scaffold for Assembly of a Pro-inflammatory "FADDosome" Complex upon TRAIL Stimulation. *Molecular Cell*, *65*(4), 715–729.e5. https://doi.org/10.1016/j.molcel.2017.01.022

Hughes, M. A., Harper, N., Butterworth, M., Cain, K., Cohen, G. M., & MacFarlane, M. (2009). Reconstitution of the Death-Inducing Signaling Complex Reveals a Substrate Switch that Determines CD95-Mediated Death or Survival. *Molecular Cell*, *35*(3), 265–279. https://doi.org/10.1016/j.molcel.2009.06.012

Hughes, M. A., Powley, I. R., Jukes-Jones, R., Horn, S., Feoktistova, M., Fairall, L., Schwabe, J. W. R., Leverkus, M., Cain, K., & MacFarlane, M. (2016). Co-operative and Hierarchical Binding of c-FLIP and Caspase-8: A Unified Model Defines How c-FLIP Isoforms Differentially Control Cell Fate. *Molecular Cell*, *61*(6), 834–849. https://doi.org/10.1016/j.molcel.2016.02.023

Irmler, M., Thome, M., Hahne, M., Schneider, P., Hofmann, K., Steiner, V., Bodmer, J. L., Schröter, M., Burns, K., Mattmann, C., Rimoldi, D., French, L. E., & Tschopp, J. (1997). Inhibition of death receptor signals by cellular FLIP. *Nature*, *388*(6638), 190–195. https://doi.org/10.1038/40657

Johnson, D. E., Burtness, B., Leemans, C. R., Lui, V. W. Y., Bauman, J. E., & Grandis, J. R. (2020). Head and neck squamous cell carcinoma. *Nature Reviews Disease Primers, 6*(92). https://doi.org/10.1038/s41572-020-00224-3

Kemmer, J. D., Johnson, D. E., & Grandis, J. R. (2018). Leveraging Genomics for Head and Neck Cancer Treatment. *https://doi.org/10.1177/0022034518756352*, *97*(6), 603–613. https://doi.org/10.1177/0022034518756352

Kim, M., Hernandez, L., & Annunziata, C. M. (2016). Caspase 8 expression may determine the survival of women with ovarian cancer. *Cell Death & Disease 2016 7:1*, *7*, e2045. https://doi.org/10.1038/cddis.2015.398

Kurppa, K. J., Liu, Y., To, C., Zhang, T., Fan, M., Vajdi, A., Knelson, E. H., Xie, Y., Lim, K., Cejas, P., Portell, A., Lizotte, P. H., Ficarro, S. B., Li, S., Chen, T., Haikala, H. M., Wang, H., Bahcall, M., Gao, Y., Shalhout. S., Boettcher, S.,

Shin, B., Thai, T., Wilkens, M., Tillgren, M., Mushajiang, M., Xu, M., Choi, J., Bertram, A., Ebert, B., Beroukhim, R., Bandopadhayay, P., Awad, M., Gokhale, P., Kirschmeier, P., Marto, J., Camaro, F., Hag, R., Paweletz, C., Wong, K., Barbie D., Long, H., Gray, N., Jänne, P. (2020). Treatment-Induced Tumor Dormancy through YAP-Mediated Transcriptional Reprogramming of the Apoptotic Pathway. *Cancer Cell*, *37*(1), 104–122.e12. https://doi.org/10.1016/j.ccell.2019.12.006

Lee, E. W., Seo, J., Jeong, M., Lee, S., & Song, J. (2012). The roles of FADD in extrinsic apoptosis and necroptosis. *BMB Reports, 45*(9), 496–508. https://doi.org/10.5483/BMBRep.2012.45.9.186

Leonard, B. C., & Johnson, D. E. (2018). Signaling by cell surface death receptors: Alterations in head and neck cancer. *Advances in Biological Regulation*, *67*, 170–178. https://doi.org/ 10.1016/j.jbior.2017.10.006

Li, C., Egloff, A. M., Sen, M., Grandis, J. R., & Johnson, D. E. (2014). Caspase-8 mutations in head and neck cancer confer resistance to death receptor-mediated apoptosis and enhance migration, invasion, and tumor growth. *Molecular Oncology*, *8*(7), 1220–1230. https://doi.org/10.1016/j.molonc.2014.03.018

Li, J., Jia, H., Xie, L., Wang, X., Wang, X., He, H., Lin, Y., & Hu, L. (2009). Association of Constitutive Nuclear Factor-κB Activation With Aggressive Aspects and Poor Prognosis in Cervical Cancer. *International Journal of Gynecologic Cancer*, *19*(8), 1421–1426. http://dx.doi.org/10.1111/IGC.0b013e3181b70445

Lowe, S. W., & Lin, A. W. (2000). Apoptosis in cancer. *Carcinogenesis*, *21*(3), 485–495. https://doi.org/10.1093/carcin/21.3.485

Maier, P., Hartmann, L., Wenz, F., & Herskind, C. (2016). Cellular Pathways in Response to Ionizing Radiation and Their Targetability for Tumor Radiosensitization. *International Journal of Molecular Sciences 2016, 17*(1), 102. https://doi.org/10.3390/IJMS17010102

Mandal, R., Barrón, J. C., Kostova, I., Becker, S., & Strebhardt, K. (2020). Caspase-8: The double-edged sword. *Biochimica et Biophysica Acta (BBA) - Reviews on Cancer*, *1873*(2), 188357. https://doi.org/10.1016/J.BBCAN.2020.188357

Orning, P., & Lien, E. (2021). Multiple roles of caspase-8 in cell death, inflammation, and innate immunity. *Journal of Leukocyte Biology*, *109*(1), 121. https://doi.org/10.1002/JLB.3MR0420-305R

Palumbo, S., & Comincini, S. (2013). Autophagy and ionizing radiation in tumors: The "survive or not survive" dilemma. *Journal of Cellular Physiology*, *228*(1), 1–8. https://doi.org/10.1002/JCP.24118

Pickering, C. R., Zhang, J., Yoo, S. Y., Bengtsson, L., Moorthy, S., Neskey, D. M., Zhao, M., Ortega Alves, M. V., Chang, K., Drummond, J., Cortez, E., Xie, T. X., Zhang, D., Chung, W., Issa, J. P. J., Zweidler-McKay, P. A., Wu, X., El-Naggar, A. K., Weinstein, J. N., Wang, J., Muzny, D. M., Gibbs, R. A., Wheeler, D. A., Myers, J. N., Frederick, M. J. (2013). Integrative genomic characterization of oral squamous cell carcinoma identifies frequent somatic drivers. *Cancer Discovery*, *3*(7), 770–781. https://doi.org/10.1158/2159-8290.CD-12-0537/

Pop, C., Fitzgerald, P., Green, D. R., & Salvesen, G. S. (2007). Role of proteolysis in caspase-8 activation and stabilization. *Biochemistry*, *46*(14), 4398–4407. https://doi.org/10.1021/BI602623B

Prasanna, A., Ahmed, M. M., Mohiuddin, M., & Coleman, C. N. (2014). Exploiting sensitization windows of opportunity in hyper and hypo-fractionated radiation therapy. *Journal of Thoracic Disease*, *6*(4), 287. https://doi.org/10.3978/J.ISSN.2072-1439.2014.01.14

Pulte, D., & Brenner, H. (2010). Changes in survival in head and neck cancers in the late 20th and early 21st century: a period analysis. *The Oncologist*, *15*(9), 994–1001. https://doi.org/10.1634/theoncologist.2009-0289

Rahmanian, N., Hosseinimehr, S. J., & Khalaj, A. (2016). The paradox role of caspase cascade in ionizing radiation therapy. *Journal of Biomedical Science*, *23*(1), 1–13. https://doi.org/10.1186/s12929-016-0306-8

Ransom, D. T., Barnett, T. C., Bot, J., De Boer, B., Metcalf, C., Davidson, J. A., & Turbett, G. R. (1998). Loss of heterozygosity on chromosome 2q: possibly a poor prognostic factor in head and neck cancer. *Head & Neck*, *20*(5), 404–410. https://doi.org/10.1002/(sici)1097-0347(199808)20:5<404::aid-hed8>3.0.co;2-1

Raudenská, M., Balvan, J., & Masařík, M. (2021). Cell death in head and neck cancer pathogenesis and treatment. *Cell Death & Disease 2021, 12*(2), 1–17. https://doi.org/10.1038/s41419-021-03474-5

Rinkel, R. N., Verdonck-de Leeuw, I. M., Doornaert, P., Buter, J., de Bree, R., Langendijk, J. A., Aaronson, N. K., & Leemans, C. R. (2016). Prevalence of swallowing and speech problems in daily life after chemoradiation for head and neck cancer based on cut-off scores of the patient-reported outcome measures

SWAL-QOL and SHI. *European Archives of Oto-Rhino-Laryngology*, *273*(7), 1849–1855. https://doi.org/10.1007/S00405-015-3680

Roos, W. P., & Kaina, B. (2013). DNA damage-induced cell death: From specific DNA lesions to the DNA damage response and apoptosis. *Cancer Letters*, *332*(2), 237–248. https://doi.org/10.1016/J.CANLET.2012.01.007

Salvesen, G. S., & Dixit, V. M. (1999). Caspase activation: the induced-proximity model. *Proceedings of the National Academy of Sciences of the United States of America*, *96*(20), 10964–10967. https://doi.org/10.1073/PNAS.96.20.10964

Sau, A., Lau, R., Cabrita, M. A., Nolan, E., Crooks, P. A., Visvader, J. E., & Pratt, M. A. C. (2016). Persistent Activation of NF-κB in BRCA1-Deficient Mammary Progenitors Drives Aberrant Proliferation and Accumulation of DNA Damage. *Cell Stem Cell*, *19*(1), 52. https://doi.org/10.1016/J.STEM.2016.05.003

Singh, R., Das, S., Datta, S., Mazumdar, A., Biswas, N. K., Maitra, A., Majumder, P. P., Ghose, S., & Roy, B. (2020). Study of Caspase 8 mutation in oral cancer and adjacent precancer tissues and implication in progression. *PLOS ONE*, *15*(6), e0233058. https://doi.org/10.1371/journal.pone.0233058

Soung, Y. H., Lee, J. W., Kim, S. Y., Jang, J., Park, Y. G., Park, W. S., Nam, S. W., Lee, J. Y., Yoo, N. J., & Lee, S. H. (2005). CASPASE-8 Gene Is Inactivated by Somatic Mutations in Gastric Carcinomas. *Cancer Research*, *65*(3), 815–821. https://doi.org/10.1158/0008-5472.815.65.3

Stein, A. P., Saha, S., Kraninger, J. L., Swick, A. D., Yu, M., Lambert, P. F., & Kimple, R. J. (2015). Prevalence of human papillomavirus in oropharyngeal cancer. *Cancer Journal*, *21*(3), 138–146. https://doi.org/10.1097/PPO.0000000000000115

Stransky, N., Egloff, A. M., Tward, A. D., Kostic, A. D., Cibulskis, K., Sivachenko, A., Kryukov, G. v., Lawrence, M. S., Sougnez, C., McKenna, A., Shefler, E., Ramos, A. H., Stojanov, P., Carter, S. L., Voet, D., Cortés, M. L., Auclair, D., Berger, M. F., Saksena, G., … Grandis, J. R. (2011). The mutational landscape of head and neck squamous cell carcinoma. *Science*, *333*(6046), 1157–1160. https://doi.org/10.1126/science.1208130

Stupack, D. G. (2013). Caspase-8 as a therapeutic target in cancer. *Cancer Letters*, *332*(2), 133–140. https://doi.org/10.1016/j.canlet.2010.07.022

Sung, H., Ferlay, J., Siegel, R. L., Laversanne, M., Soerjomataram, I., Jemal, A., & Bray, F. (2021a). Global Cancer Statistics 2020: GLOBOCAN Estimates of Incidence and Mortality Worldwide for 36 Cancers in 185 Countries. *CA: A*

Cancer Journal for Clinicians, *71*(3), 209–249. https://doi.org/10.3322/CAAC.21660

Takita, J., Yang, H. W., Chen, Y. Y., Hanada, R., Yamamoto, K., Teitz, T., Kidd, V., & Hayashi, Y. (2001). Allelic imbalance on chromosome 2q and alterations of the caspase 8 gene in neuroblastoma. *Oncogene*, *20*(32), 4424–4432. https://doi.org/10.1038/sj.onc.1204521

Teitz, T., Wei, T., Valentine, M. B., Vanin, E. F., Grenet, J., Valentine, V. A., Behm, F. G., Look, A. T., Lahti, J. M., & Kidd, V. J. (2000). Caspase 8 is deleted or silenced preferentially in childhood neuroblastomas with amplification of MYCN. *Nature Medicine, 6*(5), 529–535. https://doi.org/10.1038/75007

Teng, Y., Dong, Y. C., Liu, Z., Zou, Y., Xie, H., Zhao, Y., Su, J., Cao, F., Jin, H., & Ren, H. (2017). DNA methylation-mediated caspase-8 downregulation is associated with anti-Apoptotic activity and human malignant glioma grade. *International Journal of Molecular Medicine*, *39*(3), 725–733. https://doi.org/10.3892/ijmm.2017.2881

Tsuchiya, Y., Nakabayashi, O., & Nakano, H. (2015). FLIP the Switch: Regulation of Apoptosis and Necroptosis by cFLIP. *International Journal of Molecular Sciences*, *16*(12), 30321. https://doi.org/10.3390/ijms161226232

Tummers, B., & Green, D. R. (2017). Caspase-8: regulating life and death. *Immunological Reviews*, *277*(1), 76–89. https://doi.org/10.1111/imr.12541

Usman, S., Jamal, A., Teh, M.-T., & Waseem, A. (2021). Major Molecular Signaling Pathways in Oral Cancer Associated With Therapeutic Resistance. *Frontiers in Oral Health*. https://doi.org/10.3389/froh.2020.603160

Uzunparmak, B., Gao, M., Lindemann, A., Erikson, K., Wang, L., Lin, E., Frank, S. J., Gleber-Netto, F. O., Zhao, M., Skinner, H. D., Newton, J., Sikora, A. G., Myers, J. N., & Pickering, C. R. (2020). Caspase-8 loss radiosensitizes head and neck squamous cell carcinoma to SMAC mimetic-induced necroptosis. *JCI Insight*, *5*(23). https://doi.org/10.1172/jci.insight.139837

Wang, H. H., Wu, Z. Q., Qian, D., Zaorsky, N. G., Qiu, M. H., Cheng, J. J., Jiang, C., Wang, J., Zeng, X. L., Liu, C. L., Tian, L. J., Ying, G. G., Meng, M. Bin, Hao, X. S., & Yuan, Z. Y. (2018). Ablative Hypofractionated Radiation Therapy Enhances Non-Small Cell Lung Cancer Cell Killing via Preferential Stimulation of Necroptosis In Vitro and In Vivo. *International Journal of Radiation Oncology*Biology*Physics*, *101*(1), 49–62. https://doi.org/10.1016/j.ijrobp.2018.01.036

Watt, W., Koeplinger, K. A., Mildner, A. M., Heinrikson, R. L., Tomasselli, A. G., & Watenpaugh, K. D. (1999). The atomic-resolution structure of human caspase-8, a key activator of apoptosis. *Structure*, *7*(9), 1135–1143. https://doi.org/10.1016/S0969-2126(99)80180-4

Wong, I. C. K., Ng, Y. K., & Lui, V. W. Y. (2014). Cancers of the lung, head and neck on the rise: Perspectives on the genotoxicity of air pollution. *Chinese Journal of Cancer*, *33*(10), 476–480. https://doi.org/10.5732/cjc.014.10093

Xia, L., Tan, S., Zhou, Y., Lin, J., Wang, H., Oyang, L., Tian, Y., Liu, L., Su, M., Wang, H., Cao, D., & Liao, Q. (2018). Role of the NFκB-signaling pathway in cancer. *OncoTargets and Therapy*, *11*, 2063–2073. https://doi.org/10.2147/OTT.S161109

Zanotto-Filho, A., Gonçalves, R. M., Klafke, K., de Souza, P. O., Dillenburg, F. C., Carro, L., Gelain, D. P., & Moreira, J. C. F. (2017). Inflammatory landscape of human brain tumors reveals an NFκB dependent cytokine pathway associated with mesenchymal glioblastoma. *Cancer Letters*, *390*, 176–187. https://doi.org/10.1016/j.canlet.2016.12.015

Appendices

Appendix 1- Primer table

Primer	Sequence
KJK239 ATTL2 FW	ACCCAGCTTTCTTGTACAAA
KJK240 CASP8 flag tagging rev	TTACTTGTCATCGTCGTCCTTGTAATCATCAGAAG GGAAGACAAGT
CASP8 L7V FW	TCAGCAGAAATGTTTATGATATTGG
CASP8 L7V REV	AGTCCATGGTGGCGAAG
CASP8 L62P FW	TCCTTCCCGAAGGAGCTGC
CASP8 L62P REV	CAGATTGCTTTCCTCCAACATT
CASP8 R71T FW	GAATTAATACACTGGATTTGCTGATT
CASP8 R71T REV	GGAAGAGCAGCTCCTTCA
CASP8 S99F FW	CTCAAATTTTTGCCTACAGGG
CASP8 S99F REV	CCCTGCCTGGTGTCTGAA
CASP8 L105H FW	GGGTCATGCACTATCAGATTT
CASP8 L105H REV	TGTAGGCAGAAATTTGAGCC
CASP8 D303G FW	AACTCATGGGCCACAGTAACA
CASP8 D303G REV	GGTAGATTTTCAAAATCTCATAGATTTGC
CASP8 S375* FW	AGACTGATTAAGAGGAGCAA
CASP8 S375* REV	CAACAGGTATACCTTTCTGGTAG
CASP8 T441I FW	TATTCTCATCATCCTGACTGAA
CASP8 T441I REV	TCATCGCCTCGAGGACAT
CASP8 Q465* FW	GATGCCTTAACCTACTTTCACA
CASP8 Q465* REV	TGTTTCCCCATGTTTTTCTTGTCATC
fw-LV-RRE	TGTGCCTTGGAATGCTAGT
rev-LV-RRE	AATTTCTCTGTCCCACTCCATC